HIGH PRESSURE SOLUBILITIES AND DIFFUSION COEFFICIENTS OF CARBON DIOXIDE IN POLYETHYLENE GLYCOL 400

by
Hazal Cancı

Submitted to Graduate School of Natural and Applied Sciences
in Partial Fulfillment of the Requirements
for the Degree of Master of Science in
Chemical Engineering

Yeditepe University
2018

HIGH PRESSURE SOLUBILITIES AND DIFFUSION COEFFICIENTS OF CARBON DIOXIDE IN POLYETHYLENE GLYCOL 400

APPROVED BY:

Assoc. Prof. Betül Ünlüsü   ....
(Thesis Supervisor)

Prof. Süheyla Uzman   ....

Assoc. Prof. Kerem Uğuz   ....

DATE OF APPROVAL: ..../..../2018

ACKNOWLEDGMENTS

I would first like to thank my thesis advisor Assoc. Prof. Betül Ünlüsü for her help, suggestions and encouragement during the research and writing of this thesis.

I would like to thank the Department of Chemical Engineering at Yeditepe University.

I would like to thank my labmates Barış Emek and roommates Beril Gülkaya and Nur Çınar.

Finally, I would like to thank my family for their endless love and support, which makes everything more beautiful.

ABSTRACT

HIGH PRESSURE SOLUBILITIES AND DIFFUSION COEFFICIENTS OF CARBON DIOXIDE IN POLYETHYLENE GLYCOL 400

The aim of this study is to determine the solubilities and diffusion coefficients of carbon dioxide in polyethylene glycol 400 (PEG 400) at high pressure. Carbon dioxide forms a gas-expanded liquid system (GXL) with PEG 400 which can be used as a solvent system for biphasic reactions. During the formation of the GXL system, the mass transfer is one-way in a certain pressure range; while carbon dioxide dissolves in the liquid polymer, the polymer does not diffuse into the gas phase in measurable quantities. During the dissolution process, the liquid expands and also, its molar density changes. First, equilibrium solubilities at different pressures up to 80 bar are determined. To determine the mutual diffusivities in the system at a certain temperature and pressure, time-dependent liquid solubilities of carbon dioxide must be known. To obtain these data, the experimental set-up used consists of a pressure and temperature-monitored view-cell, high pressure syringe pump for the transfer of carbon dioxide to the cell, and a cathetometer for measuring the changes in the liquid level. A computational fluid dynamics model which accounts for the moving interface using Volume-of-fluid method and variable density is fit to the experimental data. The increase in diffusivities with the dissolution of carbon dioxide in polyethylene glycol, is determined at 80 bar and a temperature of 313.15 K.

ÖZET

KARBONDİOKSİTİN POLİETİLEN GLİKOL 400 İÇERİSİNDEKİ YÜKSEK BASINÇ ÇÖZÜNÜRLÜKLERİ VE YAYINIM KATSAYILARI

Bu çalışmanın amacı, yüksek basınçta karbondiokstin polietilen glikol 400 (PEG 400) içerisindeki çözünürlük ve difüzyon katsayılarını belirlemektir. Karbondioksit, PEG 400 ile çift-fazlı reaksiyonlar için çözücü sistemi olarak kullanılabilen bir gazla-genleştirilmiş sıvı sistemi oluşturur. Gazla- genleştirilmiş sıvı sisteminin oluşumu sırasında, kütle aktarımı belli bir basınç aralığında tek yönlüdür; karbondioksit sıvı polimerde çözünürken, polimer ölçülebilir miktarlarda gaz fazında yayınmaz. Çözünme işlemi sırasında sıvı genleşir ve ayrıca molar yoğunluğu değişir. İlk olarak, 80 bar'a kadar farklı basınçlarda denge çözünürlükleri belirlenmiştir. Sistemde belirli bir sıcaklık ve basınçta karşılıklı yayınım katsayılarını belirlemek için, karbondioksitin zamana bağlı sıvı çözünürlükleri bilinmelidir. Bu veriyi elde etmek için kullanılan deney düzeneği, basıncın ve sıcaklığın izlendiği bir yüksek basınç hücresinden, karbondioksitin hücreye aktarılmasına yarayan bir şırınga pompasından ve sıvı seviyesindeki değişiklikleri ölçmek için kullanılan bir katetometreden oluşmaktadır. Akışkan-Hacmi yöntemiyle hareketli ara-yüzeyi ve değişken yoğunluğu içeren bir hesaplamalı akışkanlar dinamiği modeli, deneysel veriye uyarlanmıştır. Polietilen glikol içinde karbondioksitin çözünmesi ile yayınma katsayılarında oluşan artış, 313.15 K'lik bir sıcaklıkta 80 bar'da belirlenmiştir.

TABLE OF CONTENTS

LIST OF FIGURES

LIST OF TABLES

LIST OF SYMBOLS / ABBREVIATIONS

D	Diffusion Coefficient
J	Diffusion Flux
P	Pressure
S	Source Term
t	Time
u	Velocity
y	Mass Fraction
x	Mole Fraction
∇x_i	Composition Gradient
V_m	Molar Volume
γ	Volume Fraction
η	Viscosity of Liquid Phase
μ	Viscosity
CFC	Chlorofluorocarbons
PEG	Polyethylene Glycol
SCF	Supercritical Fluid
VOC	Volatile Organic Solvents
VOF	Volume of Fluid

1. INTRODUCTION

PEGs have a wide range of molecular weights and complete toxicity profiles. They are mostly used in the pharmaceutical, cosmetic and food applications. There are many consumer products such as shampoos and other personal care items using this chemical. PEGs are soluble in water and their applications include aqueous solutions. They have low flammability and low vapor pressure. Recent research has focused on utilizing PEG as a solvent for various reactions employing homogeneous catalysis [1, 2].

Supercritical fluids are generally used as solvents, antisolvents or plasticizers in processing of polymers such as production of polymer composites and particles, and also polymer synthesis [3]. Carbon dioxide is one of the most preferred solvent at supercritical state since it is non-toxic, chemically-inert, non-flammable and economical. Supercritical CO_2 is a very poor solvent for polymers having high molecular weight but, its solubility in polymers is substantial in general. The solubility of CO_2 depends on processing temperature and pressure and weak interactions in the polymer [3]. The dissolved supercritical CO_2 in polymers changes the properties of the polymers such as density, viscosity and diffusivity [4].

At high pressure, CO_2 and PEGs form gas-expanded liquid systems. All liquids do not expand equally under gas pressure since there are some differences in the ability of the liquids to dissolve CO_2. Depending on this, there are three classes for liquids [5]. Class I liquids do not expand significantly. For instance, CO_2 is not soluble in water. Glycerol and other polyols are also present in this class [6]. Class II liquids such as acetonitrile, ethyl acetate, and some other organic solvents (for example, methy alcohol and hexane) dissolve large amounts of CO_2. Therefore, they have significant changes in physical properties [6]. Class III liquids dissolve smaller amounts of CO_2. Liquid polymers and ionic liquids belong to this class. During the dissolution, they expand only moderately in volume. CO_2 and PEGs form Class III gas-expanded liquid systems [6].

The purpose of this study is to determine the diffusion coefficients of carbon dioxide in polyethylene glycol 400 (PEG) at high pressure using a transport model fitted to time-dependent solubility data. The experimental setup consists of a jacketed high pressure view-cell equipped with a pressure transducer and a thermocouple, a syringe pump for carbon dioxide transfer at constant pressure, and water circulators to have constant system

temperature. The changes in the phase-interface position with the dissolution of carbon dioxide in liquid phase are measured using a cathetometer. The solubilities are calculated using the stoichiometric method [7]. ANSYS Fluent is used to model the system which consists of liquid and gas phases separated with a moving boundary. The Volume of Fluid (VOF) technique is employed to track the moving interface [7].

This thesis includes a theoretical background on polyethylene glycol (PEG) and supercritical fluids and CO_2, gas-expanded liquids and the principles of computational fluid dynamics. The experimental set-up, procedure and the transport model are explained in Section 3. Results and discussion are presented in Section 4. Finally, Section 5 consists of conclusions drawn from results and recommendations for future work.

2. THEORETICAL BACKGROUND

This section presents information on liquid polymers, supercritical fluids, gas-expanded liquids, computational fluid dynamics and previous studies about liquid polymer - carbon dioxide systems reported in the literature.

2.1. LIQUID POLYMERS

There is a growing number of studies about liquid polymers such as polyethylene glycol (PEG) and polypropylene glycol (PPG), and their copolymer PEG-PPG-PEG regarding applications in surface and colloid chemistry, and biological science [8].

PEG and PPG possess the identical spin structure of -(O-C-C)n-. Quantum mechanical calculations show the structure of -O-C-C-O- segments. There are two states in general. One state is a polar conformation and has low internal energy. The other state that has high internal energy is a nonpolar conformation [8]. The molecules of PEG or PPG may have different structures in terms of different physical states or in different chemical environments [8].

Liquid polymers exhibit nonvolatility and biodegradability. The toxicity of PEG is very low. PPG is used in facial cleansers and shampoos. Both PEG and PPG have been found as non-hazardous [9].

2.2. POLYETHYLENE GLYCOL (PEG)

Polyethylene glycol (PEG) is also called as polyethylene oxide (PEO). The chemical chain of PEG shows that methylene groups are hydrophobic while the ether oxygen and terminal hydroxyl groups are hydrophilic (see Figure 2.1). Therefore, PEG is amphiphilic [10].
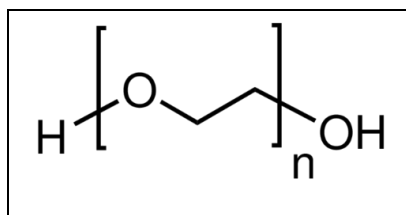
Figure 2.1. The Molecular Structure of Polyethylene glycol (PEG) [11]

Polyethylene glycol is formed with interaction of ethylene oxide and water. The acidic or basic catalysts are used for this reaction. The polymer chain length is depending on the reactants ratio [12].

$$HOCH_2CH_2OH + n(CH_2CH_2O) \rightarrow HO(CH_2CH_2O)_{n+1}H$$

Figure 2.2. The Polymerization Reaction [12]

The polymerization reaction can be cationic or anionic based on the catalyst type. The mechanism of anionic is usable in obtaining PEG with a low polydispersity. The process of polyethylene glycol synthesis is exothermic [12].

2.2.1. Properties of PEG

PEGs are soluble in water, methanol, ethanol, acetonitrile and benzene while they are insoluble in diethyl ether and hexane. The chemical structure of PEG becomes $H(OCH_2CH_2)_n$. Here, n describes the number of ethylene oxide groups. PEGs have different molecular weights that vary based on n. [13]. PEGs that have a molecular weight of 600 g/mol are liquid, while higher molecular weights become solid [14].

PEGs exhibit low flammability and vapor pressure and they are described as biodegradable, biocompatible and non-toxic. In addition, PEGs can be reprocessed and recycled from solutions to extract or distill the volatile component [15]. They behave as a co-solvent and provide the decrease of polarity in solutions. They cause an increase in the solubilities of organic molecules [15].

Although PEG is water soluble, the phase behavior is affected by the salts such as sodium hydrogen sulfate or potassium phosphate. PEGs are generally used in aqueous biphasic systems (ABSs) so, it is significant to know their phase behaviour which involves several variables such as molecular weight, presence of salts, neutral organic molecules, temperature, etc .[15].

Liquid PEGs are applied as lubricating substance in compressors and in gas cleaning with a low and high vapour pressure. Thus, it is necessary to know the phase bahavior of PEG and gases used for these applications. [16].

2.2.2. Applications of PEG

Since 1950, PEGs have been investigated as a separation and purification aid, an anti-freeze, lubricants for medical devices and food additives [17].

Liquid PEGs 200-600 may be applied as a watermiscible solubilizer in oral liquids. PEGs that possess higher molecular weight are generally applied for microencapsulation of active drug. PEGs reduce the harsh solvents use during encapsulation. PEG is also applied as a lubricant in eye drops. In addition, liquid PEGs are applied as suspending agents and emulsion stabilizers in combination [17].

2.3. SUPERCRITICAL FLUIDS

Supercritical fluids (SCFs) have gained an important role over the last 30 years. These fluids are used for separations and spectroscopic works and also for reactions and synthesis [15].

There are no limits between liquids and gases under supercritical conditions so the substance can be called as fluid. The characteristic properties of supercritical fluids are density, viscosity and diffusivity (see Table 2.1). SCFs are defined as the phase of compressible gas [18].

Table 2.1. Physical Properties [18]

Property	Density (kg/m^3)	Viscosity (cP)	Diffusivity (mm^2/s)
Gas	1	0.01	1-10
SCF	100-800	0.05-0.1	0.01-0.1
Liquid	1000	0.5-1.0	0.001

The thermodynamic properties such as volume, enthalpy, entropy and internal energy change along the vaporization curve. They are not equal for the liquid and gas phases at equilibrium. When the critical point is reached, the properties of the liquid and gas phases are equal. These phases become a single continuous phase at the critical point [19].

The critical point of a SCF presents the highest temperature and pressure at which the substance may be as a vapor and liquid at equilibrium. The three phases are coexistent at the triple point. The liquid-gas curve is represented as the boiling curve. When the temperature increases, the liquid density decreases due to thermal expansion. The gas density increases with pressure. The two phases densities converge and are the same, the difference between liquid and gas phases disappears when the boiling curve reaches to the critical point (see Figure 2.3) . This change might be observed using a high pressure view cell [15].
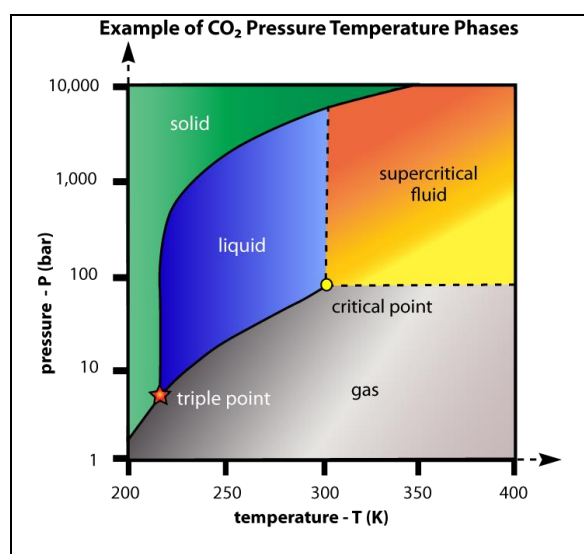

Figure 2.3. Carbon Dioxide Phase Diagram [20]

When gas-like viscosity and liquid-like density combine, they make a superb solvent for several applications. The supercritical fluids density may be fine-tuned based on the application, when the small changes are applied to pressure inside the critical region [21].

Supercritical carbon dioxide is a clean and versatile solvent. In addition, it is non-toxic, non-flammable, inactive and economical [18]. There are many advantages of using supercritical carbon dioxide ($scCO_2$) as a solvent. The advantages and disadvantages of $scCO_2$ are shown in Figure 2.4 [15].

	Advantages	Disadvantages
Environmental and safety	No liquid waste/solvent effluent Non-flammable Non-toxic to the environment/ personnel Available cheaply and in >99.9% pure form	Involves high pressures
Reaction and process	Low viscosity	Equipment costs; pressure vessels are required
	Gas miscibility	Heat transfer limitations; faster reaction rates can be problematic for particularly exothermic reactions
	Simple product isolation by evaporation to 100% dryness	Weak solvent; relatively non-polar, co-solvents or modification of reagents needed to improve solubility, but many low MWt non-polar compounds are soluble
	Range of processing techniques available, such as RESS	Reacts in the presence of good nucleophiles
	High diffusion rates offer potential for increased reaction rates	Misplaced technophobia
	Density can be varied to control reagent/product solubility, 'tunable' solvent	
	Relatively inert and non-oxidizable	

Figure 2.4. The Summary of Advantages and Disadvantages of $scCO_2$ [15]

Carbon dioxide is available in huge amounts as byproduct from the production of NH_3, H_2 and ethanol. The supercritical phase conditions are reached (Tc=304 K, Pc=7.38 MPa) and it may be taken off from a process by using depressurization process [18]. The use of $scCO_2$ in a closed cycle in large-scale processes does not form a problem for the greenhouse effect. $scCO_2$ becomes a good solvent for several nonpolar low molar mass compounds and a few polymers whereas it is usually a very poor solvent for having high molar mass polymers under the reachable conditions [22].

All gases become miscible with SCFs. SCFs additionally provides solute-solvent clustering by increasing solubility (near the critical point) as shown in Figure 2.5. [13].
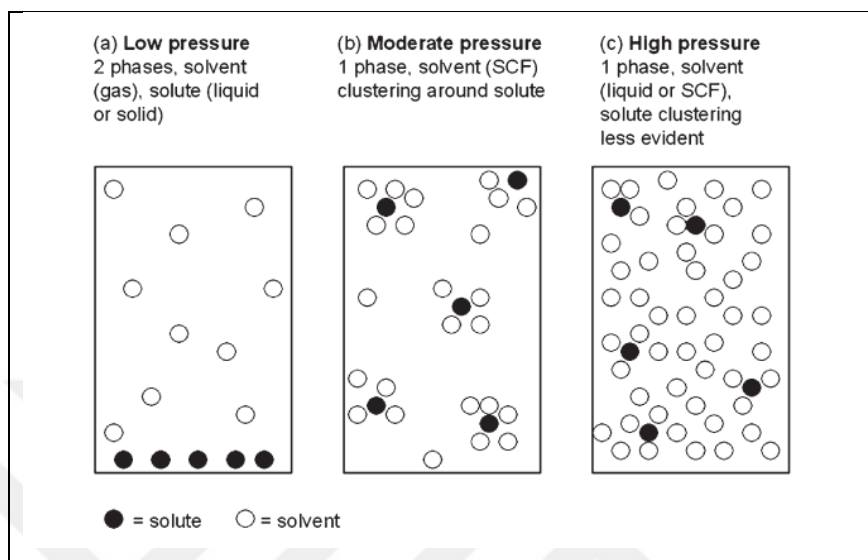

Figure 2.5. Schematic representation of solute–solvent clustering in an SCF [15]

2.3.1. Applications of Supercritical Fluids

Supercritical fluids that are used as solvents, or antisolvents or plasticizers have an important role in polymer systems such as polymer modification, polymer composites, polymer blending, microcellular foaming, and particle production. [23].

In literature, there are many applications based on extraction by using supercritical fluids. This shows that the designing of a high-pressure extraction system becomes simple at present [24]. This technology is employed for the food and pharmaceutical industries because the nontoxic nature of CO_2. In addition, this technique is used in biotechnology industries for polymer and inorganic material applications [24].

Supercritical carbon dioxide is applied in supercritical fluid extraction (SFE) and supercritical fluid chromatography (SFC). It is a good extraction solvent because it is pure, non-toxic, non-flammable, non-polar, stable, colourless, odourless and tasteless. Industrially, carbon dioxide is applied in the beverage, food and flavour, and cosmetics industries [15].

Certain advantages and disadvantages of SFE compared with other extraction techniques are indicated in Figure 2.6.

	Advantages	Disadvantages
SFE	Low-temperature extraction results in minimal degradation of volatile compounds.	Very high capital installation costs.
	Higher product yields than with steam distillation.	High running costs.
	Spent material undamaged, unlike steam distillation/solvent extraction.	Requires technically skilled operators.
		Not suitable for wet raw materials.
		Lower product yield than solvent extraction.
Steam distillation	Low capital running costs	Unpredictable degradation of some groups of compounds.
	Applicable to most essential oils, fragrances and flavour compounds.	Cleaning between products can be difficult.
	Designs available to suit all volumes.	Extraction of further products from residue can be difficult due to high moisture level.
Solvent extraction	Non-selective; wide spectrum of compounds extracted simultaneously (that can be a disadvantage too).	Most solvent residues must be monitored and tightly controlled.
	Extraction carried out at various temperatures and pressures.	Most commonly used solvents are highly flammable and possibly toxic.
	Solvents can be readily removed at atmospheric or reduced pressure.	Waste has little or no value.

Figure 2.6. Advantages and Disadvantages of Supercritical Fluids [15]

Supercritical fluids are used as reaction media, in particles formations, fibers and substrates or in drying materials [15].

2.4. GAS EXPANDED LIQUIDS (GXLs)

Investigations on GXLs have grown rapidly in the last 20 years. When a condensable gas like CO_2 pressurises a liquid, volume of liquid increases. This formed liquid-gas system is called a GXL (see Figure 2.7).
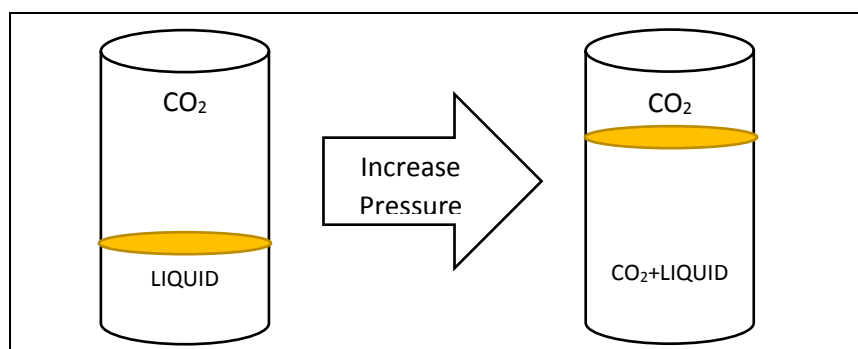
Figure 2.7. Gas-Expanded Liquid Formation

There are some different behaviors of liquids with expanding gases. This system classification has been offered by Jessop et al [25].

- Class I: the gas has a low solubility in the liquid, and the liquid does not expand much such as CO_2+H_2O.

- Class II: the solubility of the gas is high and the expansion is large such as $CO_2+Methanol$.

- Class III: GXLs are liquids where the gas is soluble but the expansion is not that large such as CO_2+ionic liquids or liquid polymers.

Jessop et al., describes a GXL as "a mixed solvent composed of a compressible gas dissolved in an organic solvent" [25]. Eckert et al. suggests that a CO_2-expanded liquid (CXL) can be a CO_2 mixture and an organic solvent at conditions under the mixture critical point [25].

The definition of Eckert et al. involves the mixtures that have low pressure and high temperature, but Jessop et al. accept that an enhanced fluidity liquid (EFL) has resemblance to a liquid more closely than a SCF because, at high pressures, an EFL compressibility is much less than a SCF (see Figure 2.8) [25].

A GXL is a condensible gas mixture. There are only two fluid phases or one phase on the bubble point curve but under the critical composition where the liquid phases properties differ from those at atmospheric pressure. This rules out mixtures that are next to the dew point curve, but contains mixtures where the components are solid at atmospheric pressure [25].
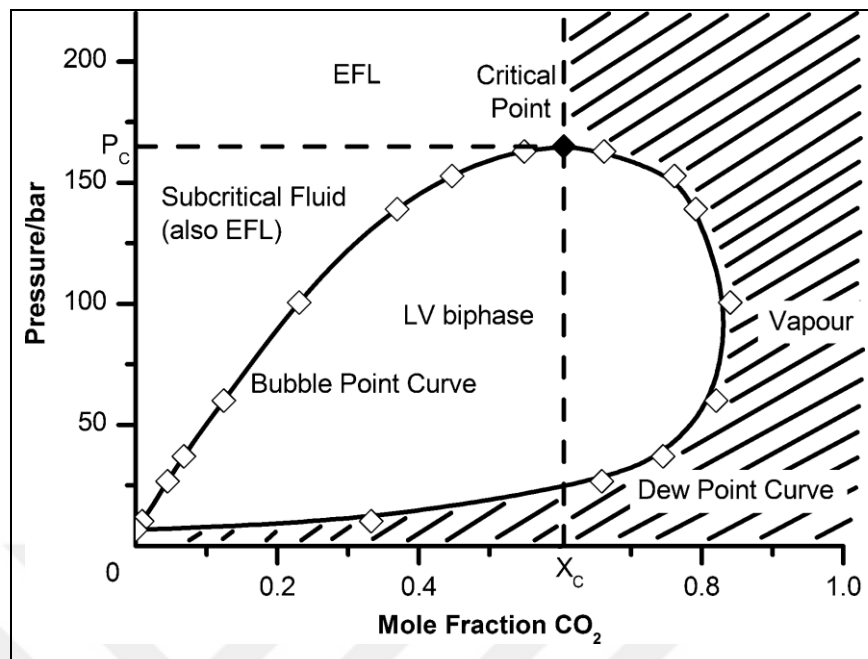
Figure 2.8. Different Phase Region [25]

When CO_2 is applied as the gas, the result is described as a carbon dioxide-expanded liquid (CXL). In addition, the dissolved CO_2 increases the diffusivity in the CXL phase and reduces the liquid phase viscosity [26].

2.4.1. Carbon dioxide-Expanded Liquids

CO_2–PEG solutions are applied to particle formation processes, biphasic reaction systems and membrane materials for gas separations [27].

In biphasic systems, one phase immobilizes the catalyst while the other phase behaves as a mobile phase for delivering reactants and removing products based on the phase equilibrium conditions. As shown in Figure 2.9, the biphasic system must have the characteristics of no cross contamination of the phases and no catalyst partitioning [28].
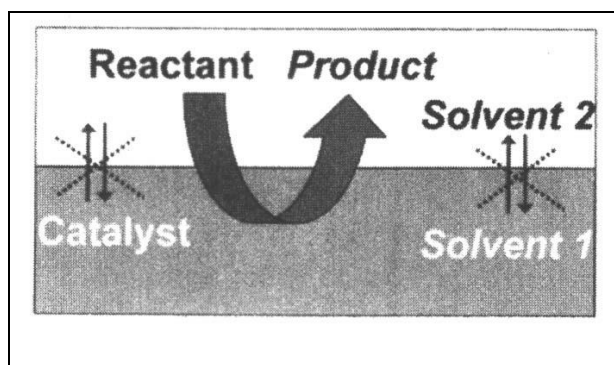
Figure 2.9. Multiphase Catalysis System [28]

The biphasic polyethylene glycol and compressed carbon dioxide process can provide these properties. The dissolution of PEG 400 in CO_2 can be prevented using an appropriate processing pressure. On the other hand, CO_2 will be soluble in the liquid polymer and will help transfer of reactants to this phase based on thermodynamic equilibrium conditions valid for the selected pressure and temperature. [28].

2.5. CARBON DIOXIDE AND POLYMER SYSTEMS

The CO_2 solubility in polymers is affected by pressure, temperature, molecular weight, polydispersity of the polymer, van der Waals interactions between the polymer and CO_2. Thus, the models of thermodynamics for CO_2 and polymer processes include all these interactions for the designing and optimizing of polymer systems [29].

The supercritical CO_2 applications in polymer systems plays a significant role in terms of the interactions with polymers and monomers. Generally, there are intermolecular forces between the molecules or polymer segments depending on the thermodynamic properties. The interactions which occurs are dispersion, dipole-dipole, dipole-quadrupole, and quadrupole-quadrupole [30].

The gas solubility in molten polymers is important in many industries for the supercritical and polymer systems. The supercritical CO_2 in molten polymers changes several physical properties of the polymers such as the viscosity, diffusivity and density [30].

When pressure increases, the gas solubility increases in a solvent. The same law is usable for CO_2 and polymer systems. The CO_2 density depending on the temperature and pressure has a major effect on the solubility in a polymer but, the amount of CO_2 which dissolves in different polymers varies based on the chemical groups. [30].

Daneshvar et. al. presented the phase equilibrium data of polyethylene glycol with different molecular weights and carbon dioxide mixtures and these data were correlated by using a lattice model. This process was carried out at temperatures of 313 K and 323 K and at pressures up to 29 MPa. [31]. Tables 2.2 and 2.3 show the phase equilibrium data for PEG 400-CO_2 systems in terms of liquid CO_2 mole fraction [31].

Table 2.2. Thermodynamic Phase Equilibrium Data for CO_2-PEG 400 (313.15K)

	1.46 MPa	3.00 MPa	6.49 MPa	7.94 MPa
Daneshvar et.al.	0.19	0.36	0.58	0.78

Table 2.3. Thermodynamic Phase Equilibrium Data for CO_2-PEG 400 (323.15K)

	1.92 MPa	4.06 MPa	7.15 MPa	8.31 MPa
Daneshvar et.al.	0.13	0.25	0.41	0.53

Gourgoouillon et. al. obtained the phase equilibrium data for PEG with different molecular weights, PEG 200-600, with scCO2. The work was carried out at temperature of 313-348 K and pressures up to 26 MPa. [32]. Tables 2.4 and 2.5 show the solubilities in terms of carbon dioxide mole fractions .

Table 2.4. Thermodynamic Equilibrium Data for PEG 400 (313.15K)

	5.23 MPa	10.62 MPa	16.11 MPa	19.74 MPa	24.01 MPa
Gourgouillon et.al.	0.60	0.75	0.77	0.78	0.8

Table 2.5. Thermodynamic Equilibrium Data for PEG 400 (333.15K)

	5.28 MPa	10.37 MPa	14.98 MPa	20.63 MPa	24.62 MPa
Gourgouillon et.al.	0.49	0.67	0.73	0.75	0.77

Li et. al. have obtained CO_2 solubilities in polyethylene glycols with molecular weights of 150, 200, 300, and 400 from 100 to 1200 kPa and from 303.15 to 333.15 K. [33] (See Tables 2.6 and 2.7).

Table 2.6. Thermodynamic Equilibrium Data (313.15K)

	166.0 kPa	300.5 kPa	414.4 kPa	578.0 kPa	834.5 kPa	1087.5 kPa
Li et.al.	0.0279	0.0567	0.0759	0.1027	0.1467	0.1905

Table 2.7. Thermodynamic Equilibrium Data (323.15K)

	154.1 kPa	217.4 kPa	443.0 kPa	564.0 kPa	893.8 kPa	1120.5 kPa
Li et.al.	0.0237	0.0333	0.0690	0.0877	0.1362	0.1701

2.6. COMPUTATIONAL FLUID DYNAMICS

Today, Computational Fluid Dynamics (CFD) methods are defined in several textbooks and used in engineering science. They have an important role for designing and engineering of components and systems in turbo machinery and aerospace [34].

Engineers carry out experiments and analyses of CFD and the two complement each other. They find global properties like lift, drag, pressure drop. However, they apply CFD to get details about the shear stresses, velocity and pressure profiles [35].

While CFD may solve laminar flows with ease, the solution is more difficult for turbulent flows [33].

Equation 2.1 is the conservation of mass equation for incompressible flow [35].

$$\vec{\nabla}.\vec{V}=0 \tag{2.1}$$

Equation 2.2 is the transport equation.

$$(\vec{V}.\vec{\nabla})\vec{V}=-\frac{1}{\rho}\vec{\nabla}P'+\nu\nabla^2\vec{V} \tag{2.2}$$

$\vec{V}$ is the fluid velocity, ρ is its density, and υ is its kinematic viscosity. Equation 2.1 and 2.2 are only applied for incompressible flow, ρ and υ are accepted constant. [35].

For solving equations 2.1 and 2.2, a computational domain is selected and a mesh is formed. The domain is divided in several small cells. The cells are areas for two dimensional domains and they are volumes for three dimensional domains (see Figure 2.10). Boundary conditions are set on each of the computational domain edge (2-D flows) or on each domain face (3-D flows). Numerical parameters and solution algorithms are chosen. Initial conditions are important as a beginning point. Then, the iteration process starts. When the solution has converged, the variables of flow field like velocity and pressure are shown graphically. Global properties like pressure drop and integral properties like forces and moments are found from the converged solution [35].
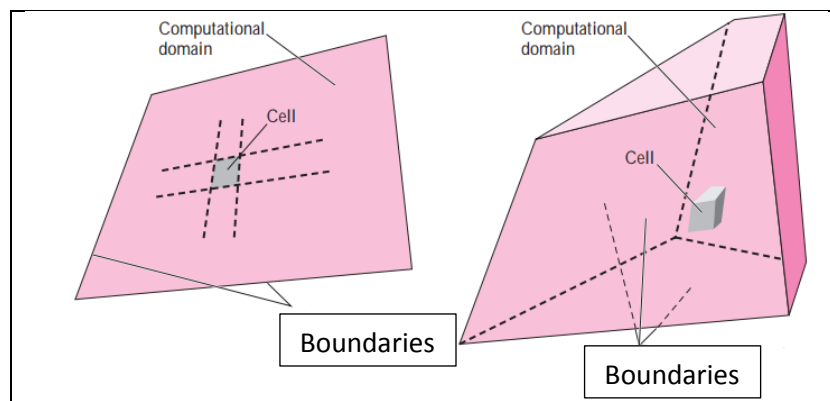

Figure 2.10. Computational Domain [35]

Some of the applications of the numerical simulations of fluid flow are the following:

- to develop the aerodynamic characteristics by vehicles designers
- to plan optimal oil recovery strategies by petroleum engineers
- to predict the weather patterns by meteorologists
- to decrease radiation risks

In computational fluid dynamics, the volume of fluid method (VOF) is a numerical technique for tracking fluid-fluid interfaces. The VOF method is defined on a concept of a fractional volume of fluid that is described by a function F. The evolution of the F field is shown by the following transport equation [36].

$$\frac{\partial F}{\partial t} + \frac{\partial uF}{\partial x} + \frac{\partial vF}{\partial y} + \frac{\partial wF}{\partial z} = 0 \tag{2.3}$$

t : physical time

x, y, z : cartesian system

u, v, w : cartesian components of the velocity

3. EXPERIMENTAL SET-UP AND TRANSPORT MODEL

In this part, the experimental set-up, procedure and transport model are described in detail.

3.1. EXPERIMENTAL SET-UP AND PROCEDURE

The system consists of the following equipments

- Jerguson high pressure view-cell
- ISCO 260 D syringe pump
- Cathetometer
- Pressure transducer
- Thermocouple
- Water circulators

Figure 3.1. Experimental Set-Up

In Figure 3.2, ISCO high pressure syringe pump is shown. The syringe pump supplies precise, predictable flow and pressure control at flow rates. The D-series controller has a

keypad and LCD display. -The ISCO pump is run at constant pressure mode during the diffusion experiments [37];

Figure 3.2. ISCO High Pressure Syringe Pump

Figure 3.3 indicates the high pressure Jerguson view-cell. Jerguson Reflex Level Gages are ideal for level indication applications [38].
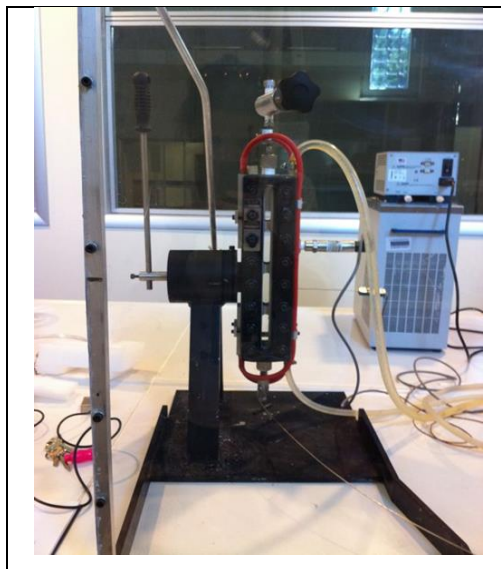

Figure 3.3. Jerguson High Pressure Cell

The cathetometer is used for the measurement of vertical distances (e.g. level differences, liquid levels etc.). It consists of a vertical column with a millimeter scale. On the column a slider carrying a telescope with horizontal optical axis can be adjusted. The slider has a scale for reading off level differences with an accuracy of 0.01 millimeters [39].

Figure 3.4. Cathetometer

The experiments start with cooling the ISCO high pressure pump down to $10^{\circ}C$ and filling it with liquid CO_2. Then, temperature and pressure of the pump are increased. the system is checked for the leaks before the experiment.

First, Jerguson view- cell is loaded with CO_2 at high pressure and then the inlet valve is closed. The inside pressure is monitored. After that, the inlet valve is opened again and the ISCO-Jerguson line is tested. At the end of the test, Jerguson is depressurized.

Polyethylene glycol (PEG400) is injected into the view-cell from the lower valve and the cathetometer is set to zero at the liquid-vapor interface.

The pressure is set to the desired experimental value. Then the outlet valve of ISCO is opened and the line is filled with carbon dioxide and the initial volume reading is taken. Later, the inlet valve of the view-cell is opened and the dissolution process gets started with carbon dioxide loading.

Temperature, pressure, polyethylene glycol(PEG 400) - CO_2 interface height and the amount of CO_2 remaining in the syringe pump are recorded until equilibrium. Then the system is depressurized.

The polyethylene glycol (PEG400) is removed from the view-cell which is washed with ethanol and left for drying at 70 °C.

3.2. THE TRANSPORT MODEL

Adding high pressure carbon dioxide to PEG generates one-way mass transfer where carbon dioxide diffuses into the liquid phase but PEG does not transfer to the gas phase. Thus, this system has two phases separated with a moving boundary (see Figure 3.5)
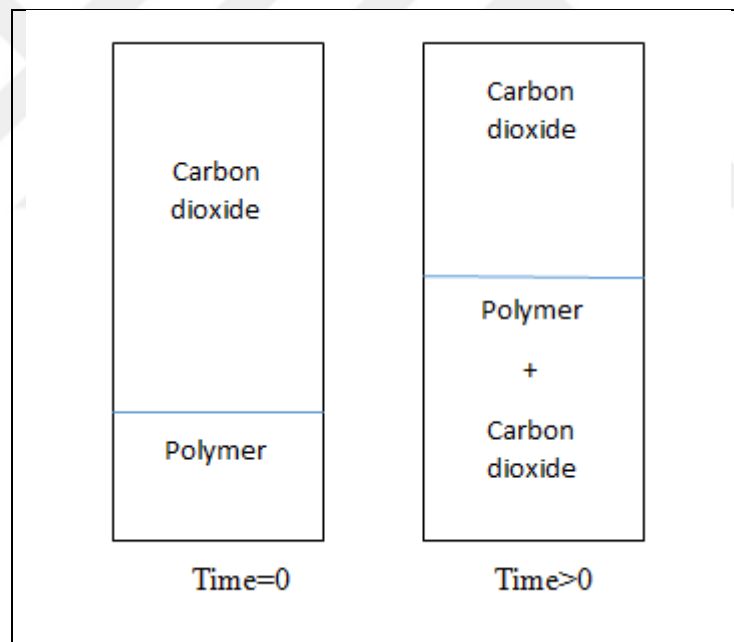
Figure 3.5. Model of Ionic Liquid- Carbon dioxide System

ANSYS Fluent is employed for modeling this system. The Volume of Fluid (VOF) technique is used in Fluent to express the moving interface. Eq. 3.1 is utilized for the advection of phase interphase by the velocity field:

$$\frac{1}{\rho_q}\frac{\partial(\alpha_q\rho_q)}{\partial t}+\nabla.\left(\alpha_q\rho_q u\right)=S_{\alpha q} \tag{3.1}$$

Here,

- ρ: density
- u: velocity of q phase

$\alpha_q=0$ when there is no q phase in a cell.

$\alpha_q=1$ when there is only q phase.

$0<\alpha_q<1$, when the interfce is in the cell.

The source term ($S_{\alpha q}$) has a value other than 0 as a result of mass transfer between phases. The source term for transfer of mass to liquid phase is calculated using Eq. 3.2. The gas phase will lose an equal amount of mass (see Eq. 3.3).

$$S_{\alpha L}=-\rho_L D\nabla y^{CO_2}.\nabla\alpha_L \tag{3.2}$$

$$S_{\alpha G}=-S_{\alpha L} \tag{3.3}$$

Eq. 3.4 shows the momentum equation.

$$\frac{\partial(\rho u)}{\partial t}+\nabla.(\rho uu)=-\nabla P+\mu\nabla^2 u+\rho g \tag{3.4}$$

Eq. 3.5 decribes the transport of carbon dioxide.

$$\frac{\partial(\rho_q\alpha_q y_q^{CO_2})}{\partial t}+\nabla.\left(\rho_q\alpha_q u y_q^{CO_2}\right)=-\nabla\left(\alpha_q J_q^{CO_2}\right)+S^{CO_2} \tag{3.5}$$

$$J^{CO_2}=-D\nabla(\rho y^{CO_2}) \tag{3.6}$$

- $y_q^{CO_2}$: the mass fraction of carbon dioxide in the qth phase
- $J_q^{CO_2}$: the diffusion flux of carbon dioxide in this phase
- S^{CO_2} : the source term for carbon dioxide

As seen in equation 3.2, while calculating mass transfer between phases, mass fraction gradient is needed at the phase interface.Thus, in Fluent, transport equations for components are solved separately for each phase. Therefore, a discontinuity in the liquid carbon dioxide mass fraction gradient occurs at the interface and mass transfer value is physically wrong here. A user defined scalar (φ) for the entire flow domain is defined to overcome this problem. The scalar shared by both phases and the following transport equation is solved for the whole domain.

$$\frac{\partial(\rho\varphi_k)}{\partial t}+\nabla.\left(\rho u\varphi_k\right)=-\nabla.\left(J_{\varphi k}\right)+S_{\varphi k} \tag{3.7}$$

The value of the scalar is equal to the mass fraction at the interface in each of the cells filled with the gas phase. These cells need to keep the same mass fraction and to ensure this, a method, called internal boundary condition, is used, where the transport equation is made dominated by a source term, defined in equation 3.8, which is given an exceptionally large value in the gas phase but, the source term is given zero in the liquid phase .

$$S_{\varphi k} =A\left(\varphi_{k,eq}-\varphi_k\right) \tag{3.8}$$

$$J_{\varphi}=-\rho_L D\nabla y_{CO_2} \tag{3.9}$$

User-defined functions are used for the source terms, liquid phase density and diffusivity.The computations are run with the grid number 2000 [7].

4. RESULTS AND DISCUSSION

In this study, solubilies of CO_2 in PEG 400 at different pressures and mutual diffusion coefficients for PEG 400-CO_2 system are determined. The change in the binary diffusivities with the liquid mole fraction of carbon dioxide are examined at 80 bar and at a temperature of 313.15. The decrease in molar volumes during the diffusion process and the change in liquid levels are reported.

The CFD model explained in the previous section is fitted to the experimental time-dependent solubility data using a trial and error approach. The diffusivity valid for all the cells in the computational domain is changed until the numerical result matches with the experimental data point. This procedure is repeated for all the experimental data points collected during the diffusion process.

4.1. THE SOLUBILITY OF CO_2 IN PEG 400 AT 313.15 K AND DIFFERENT PRESSURES (30-80 BAR)

Five experiments at different pressures have been carried out. At 313.15 K, the equilibrium mole fractions of carbon dioxide in PEG 400 are presented in Table 4.1. We observe that the solubilities increase with pressure whereas the molar volumes decrease. The collected experimental data are shown in Table 4.2.

Table 4.1. Equilibrium Mol Fractions of CO_2 and Liquid Molar Volumes at Different Pressures (313.15 K)

P(bar)	x_{CO_2}	V_{molar}
0	0	0
30	0.367	255.3
40	0.491	207.1
50	0.563	180.7
62	0.660	150.3
80	0.661	147.8

Table 4.2. Experimental Data For Solubility (313.15 K)

Pressure of the system during the experiment	30 bar	40 bar	50 bar	62 bar
Mass of the PEG 400 in the system	8.4218 g	8.2724 g	8.4129 g	8.2239 g
Volume of carbon dioxide loaded to the system	144.44 mL	122.68 mL	143.88 mL	146.72 mL
Initial volume of carbon dioxide in syringe pump	202.78 mL	211.07 mL	248.01 mL	196.25 mL
Final volume of carbon dioxide in syringe pump	51.06 mL	78.6 mL	95.81 mL	41.05 mL

In the phase equilibrium experiments, since the final mole fractions are significant, the system is left to reach equilibrium overnight and the intermediate data are not collected. Figures 4.1-4.4 show that the mole fraction of carbon dioxide increases in the liquid with

time and eventually reaches equilibrium. In Figure 4.5, the data are collected for the entire duration of the experiment to be able to carry out diffusivity calculations.
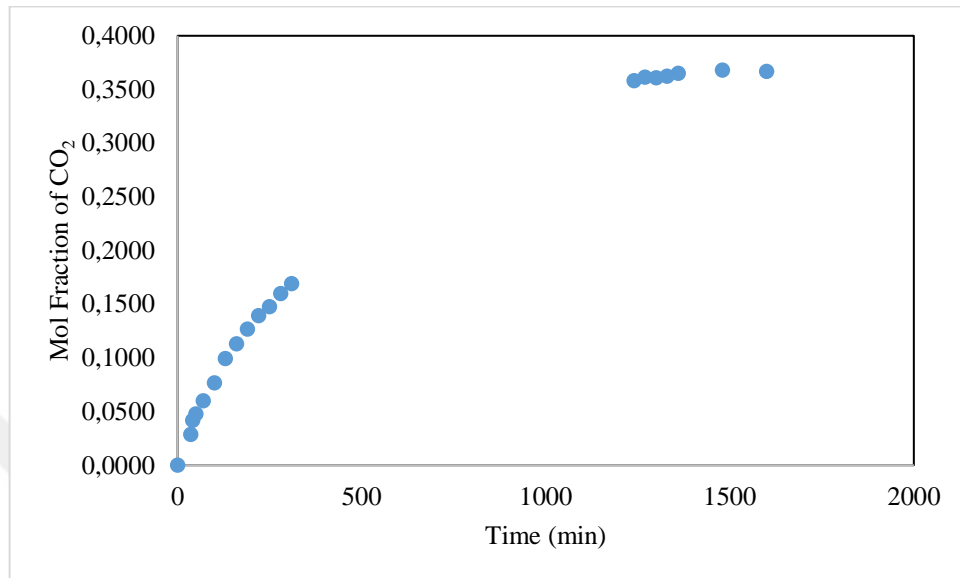
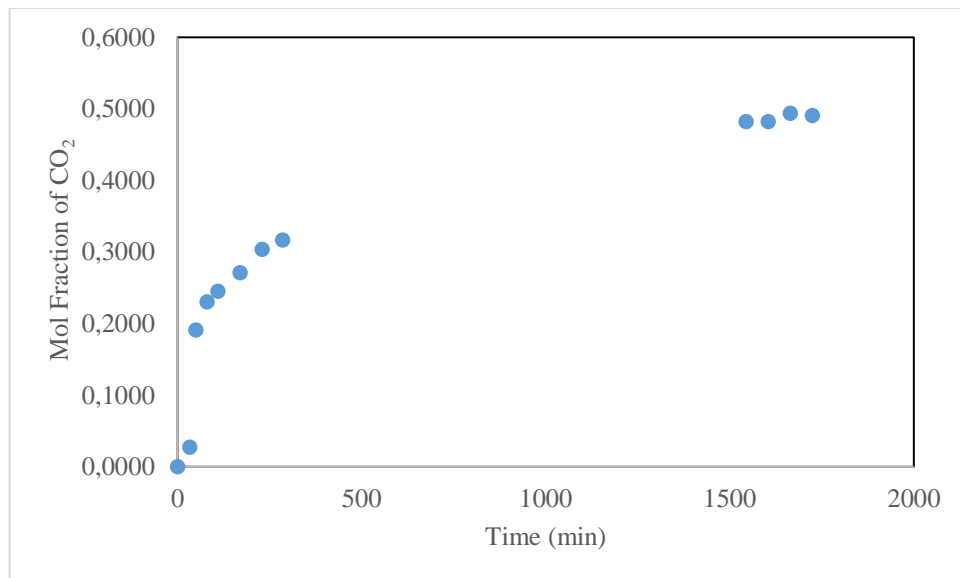Figure 4.1. Change in Liquid Mol Fraction of CO_2 with Time at 30 bar, 313.15 K

Figure 4.2. Change in Liquid Mol Fraction of CO_2 with Time at 40 bar, 313.15 K
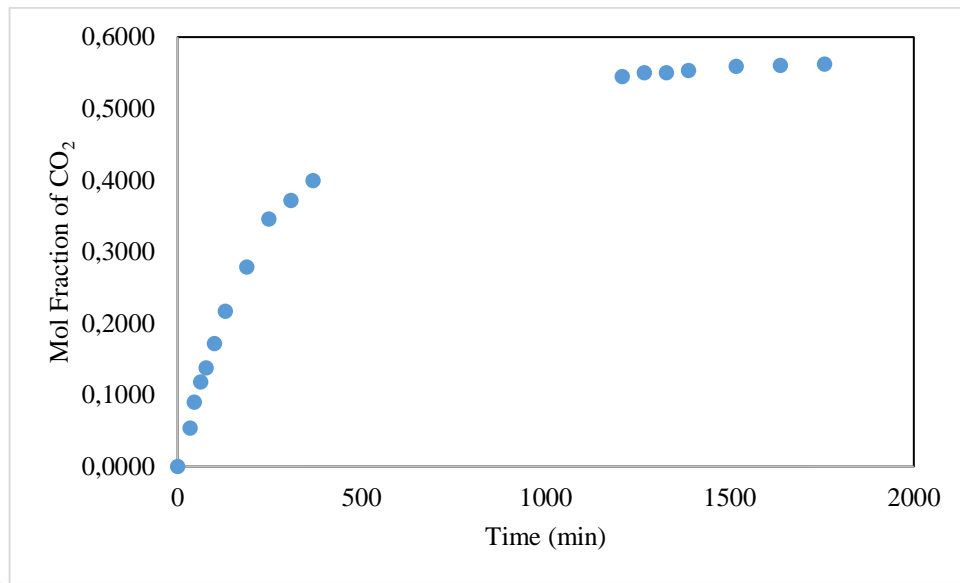
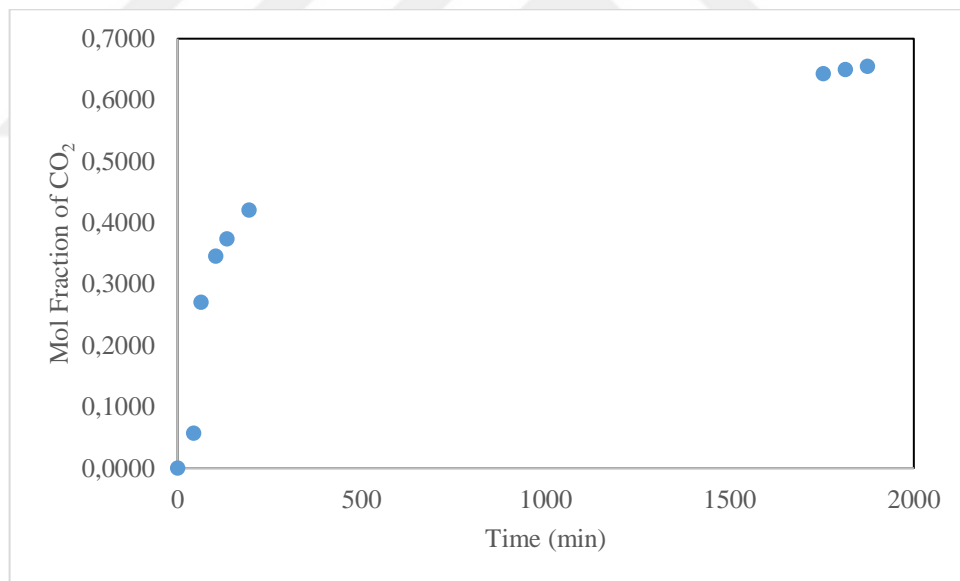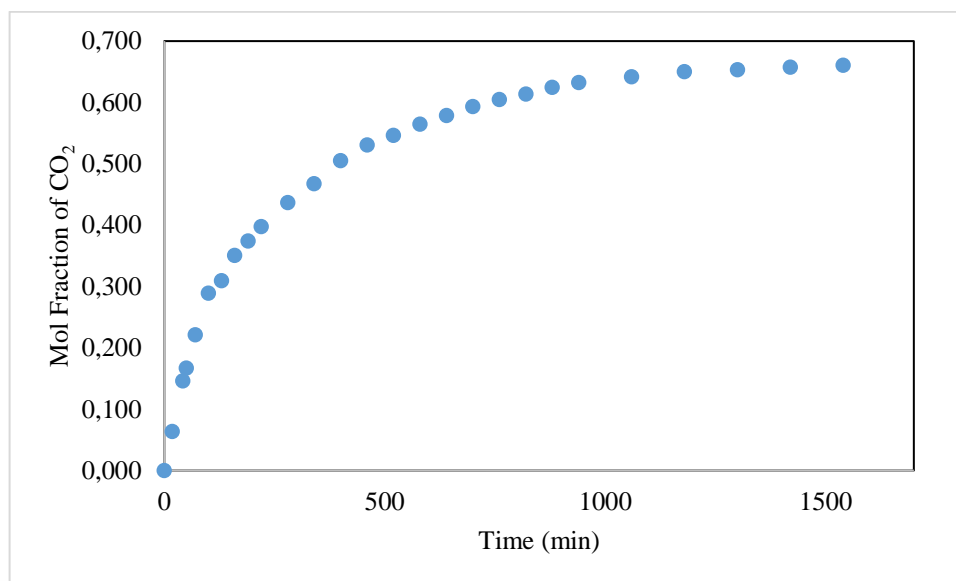Figure 4.3. Change in Liquid Mol Fraction of CO_2 with Time at 50 bar, 313.15 K

Figure 4.4. Change in Liquid Mol Fraction of CO_2 with Time at 62 bar, 313.15 K

Figure 4.5. Change in Liquid Mol Fraction of CO_2 with Time at 80 bar, 313.15 K

Our results are more comparable to data presented by Gourgouillon et. al. (Table 2.4) whereas the data reported by Daneshvar et. al. (Table 2.2) are higher.

4.2. THE SOLUBILITY OF CO_2 IN PEG 400 AT 323.15 K AND DIFFERENT PRESSURES (30-80 BAR)

At 323.15 K, the liquid equilibrium mole fractions of carbon dioxide at different pressures are presented in Table 4.3. Table 4.4 shows the experimental data. The solubilities are slightly higher at 313.15 K compared to 323.15 K as shown in Figure 4.6.

Table 4.3. Equilibrium Mol Fractions of CO_2 and Liquid Molar Volumes at Different Pressures (323.15 K)

P(bar)	x_{co2}	V_{molar}
0	0	0
30	0.351	256.6
40	0.460	219.2
50	0.520	199.7
62	0.562	187.6
80	0.605	174.4

Table 4.4. Experimental Data For Solubility (323.15 K)

Pressure of the system during the experiment	30 bar	40 bar	50 bar	62 bar
Mass of the PEG 400 in the system	8.4248 g	7.9984 g	8.4519 g	8.4040 g
Volume of carbon dioxide loaded to the system	142.8 mL	144.93 mL	144.19 mL	82.08 mL
Initial volume of carbon dioxide in syringe pump	194.26 mL	228.62 mL	202.99 mL	202.99 mL
Final volume of carbon dioxide in syringe pump	42.43 mL	75.93 mL	51.09 mL	114.16 mL
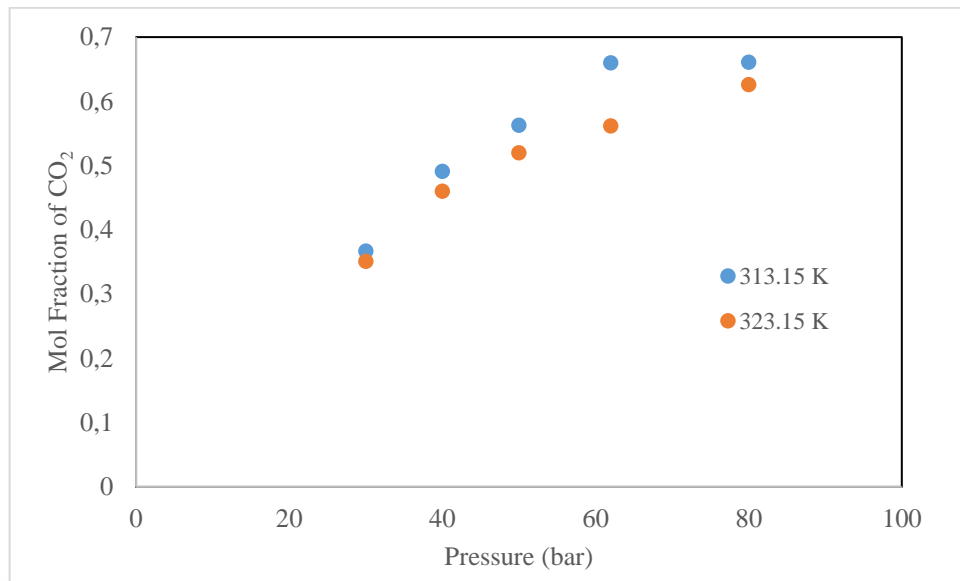
Figure 4.6. Equilibrium CO_2 Mol Fraction at Different Temperatures

Figures 4.7-4.11 show the change in CO_2 mole fractions with time. As explained for the experiments carried out at 313.5 K, after the initial solubility data, the system is left to reach equilibrium and the final data points are collected.
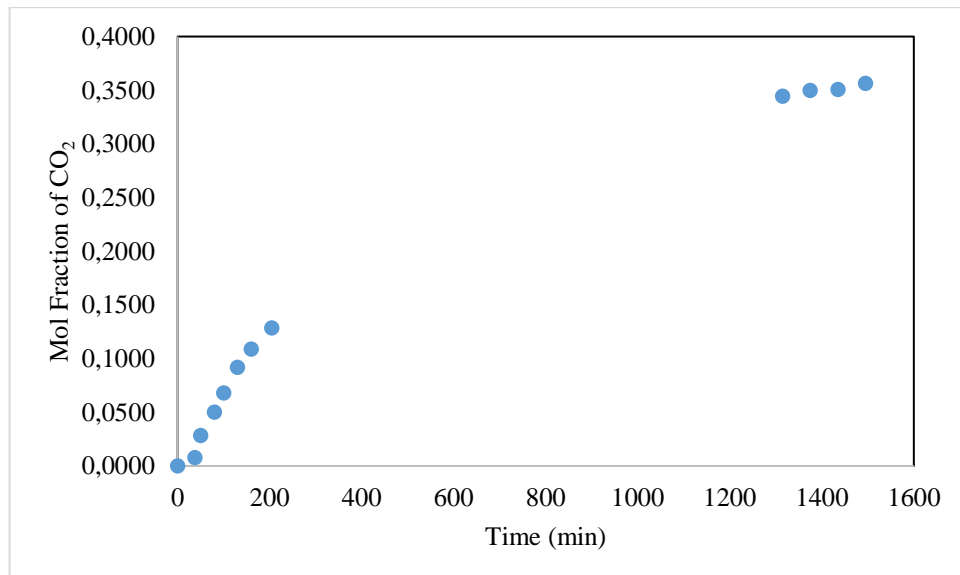

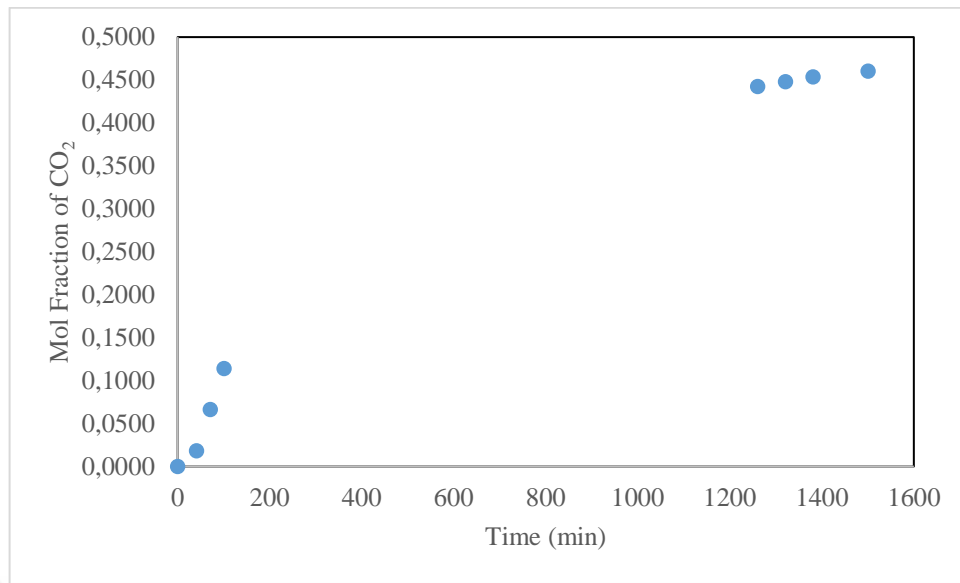Figure 4.7. Change in Liquid Mol Fraction of CO_2 with Time at 30 bar, 323.15 K

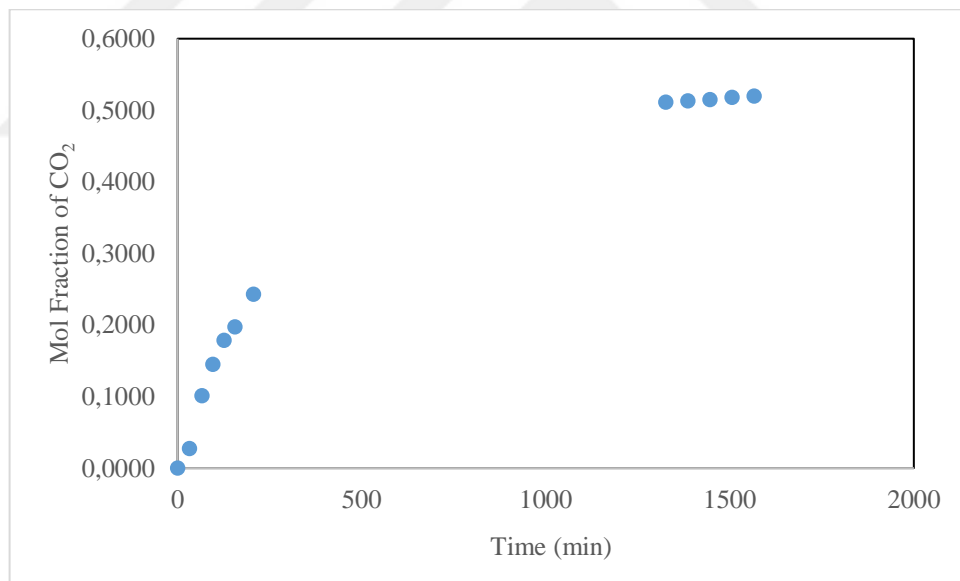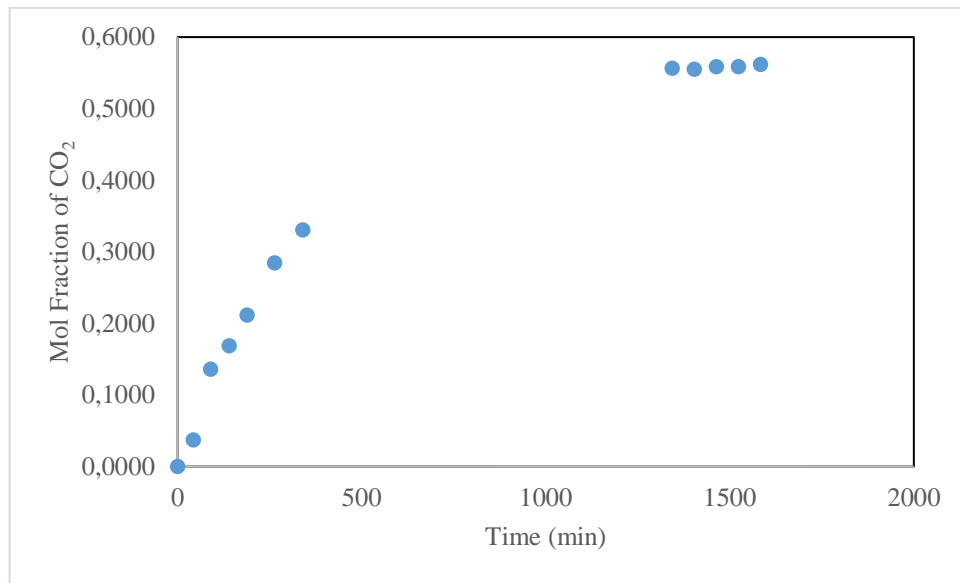Figure 4.8. Change in Liquid Mol Fraction of CO_2 with Time at 40 bar, 323.15 K

Figure 4.9. Change in Liquid Mol Fraction of CO_2 with Time at 50 bar, 323.15 K

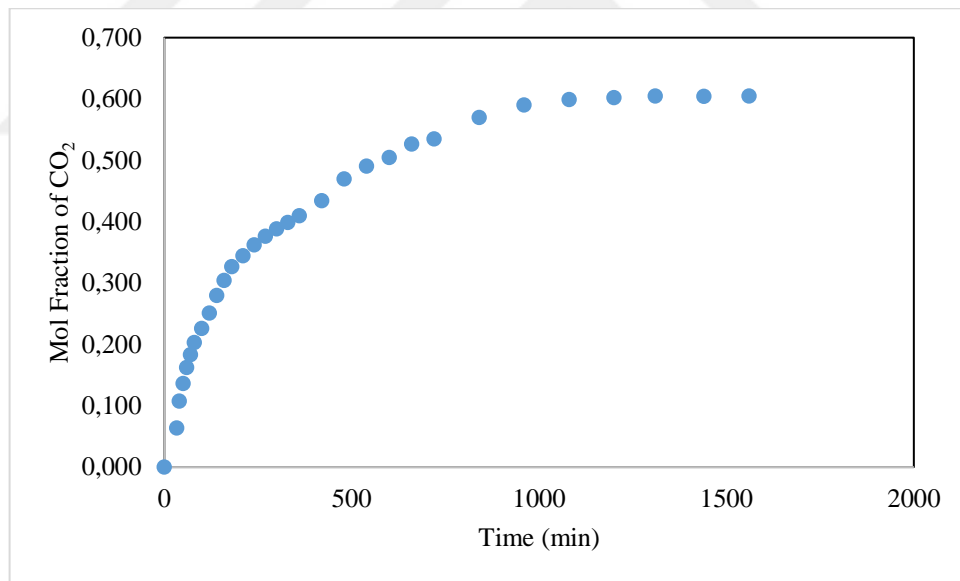Figure 4.10. Change in Liquid Mol Fraction of CO_2 with Time at 62 bar, 323.15 K

Figure 4.11. Change in Liquid Mol Fraction of CO_2 with Time at 80 bar, 323.15 K

The repeat experiments are presented in Appendices A, B and C.

4.3. PEG 400 – CO₂ SYSTEM AT 313.15 K AND 80 BAR

The experimental data is shown below. The mol fraction is found as 0.66 at equilibrium. This value is found by using the increase in the liquid level measured using the cathetometer, and the volume reading from the syringe pump. A sample calculation for the mol fraction in equilibrium is indicated in Appendix D.

Table 4.5. The Experimental Data for 80 bar, 313.15 K

Mass of the PEG 400 in the system	8.2713 g
Volume of carbon dioxide loaded to the system	143.96 ml
Initial volume of carbon dioxide in syringe pump	245.75 ml
Final volume of carbon dioxide in syringe pump	97.5 ml
Increase in liquid level	3.04 mm
Pressure of the system during the experiment	80 bar
Temperature of the system during the experiment	313.15 K

Figure 4.12 shows the experimental and modeling results. Different diffusivity values in the user-defined functions are tried until the mol fraction of CO_2 numerically fits the experimental data at different times. Thus, a single average value for the diffusivity valid at a certain time is found.

Molar volume changes linearly with mole fraction as shown in Figure 4.13. The linear equation shown in the figure is used in the program to take the molar volume change into account. Figure 4.14 shows that as carbon dioxide dissolves in the liquid, molar volume decreases.
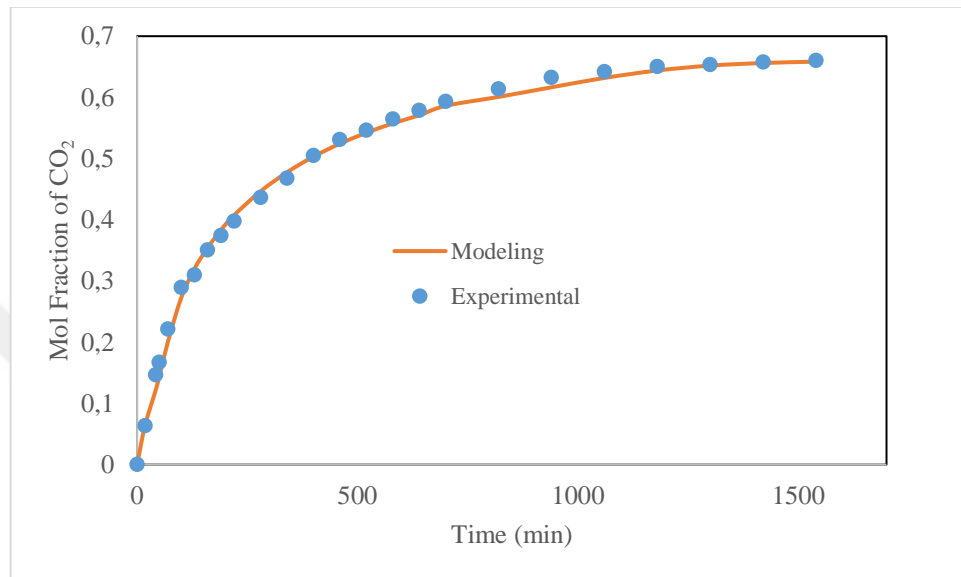

Figure 4.12. Modeling and Experimental Results for the Changing Mol Fraction of CO_2 with Time at 80 bar, 313.15 K
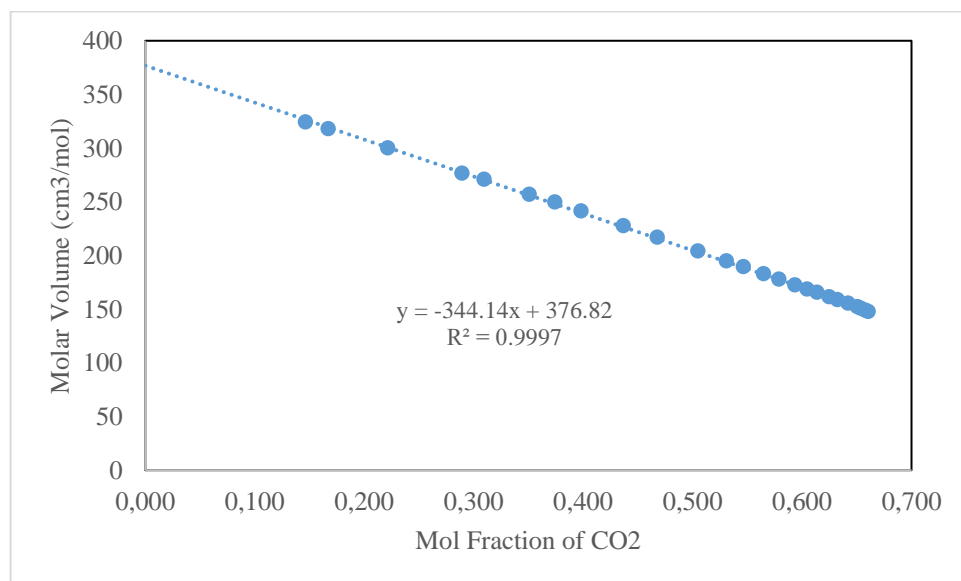

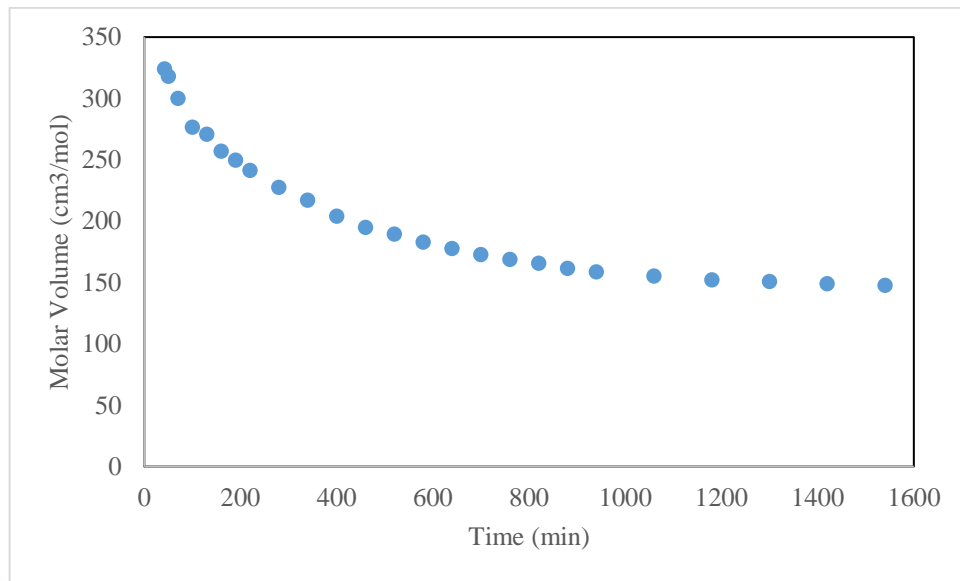Figure 4.13. Change in the Molar Volume with Mole Fraction of Carbon dioxide at 80 bar, 313.15 K

Figure 4.14. Change in Liquid Molar Volume with Time at 80 bar, 313.15 K

Figure 4.15 shows the calculated diffusivity values which have increased with the mole fraction of carbon dioxide in the liquid. The diffusivity starts from 3.2×10^{-10} m^2/s and increases to 19.2×10^{-10} m^2/s until the end of the process.
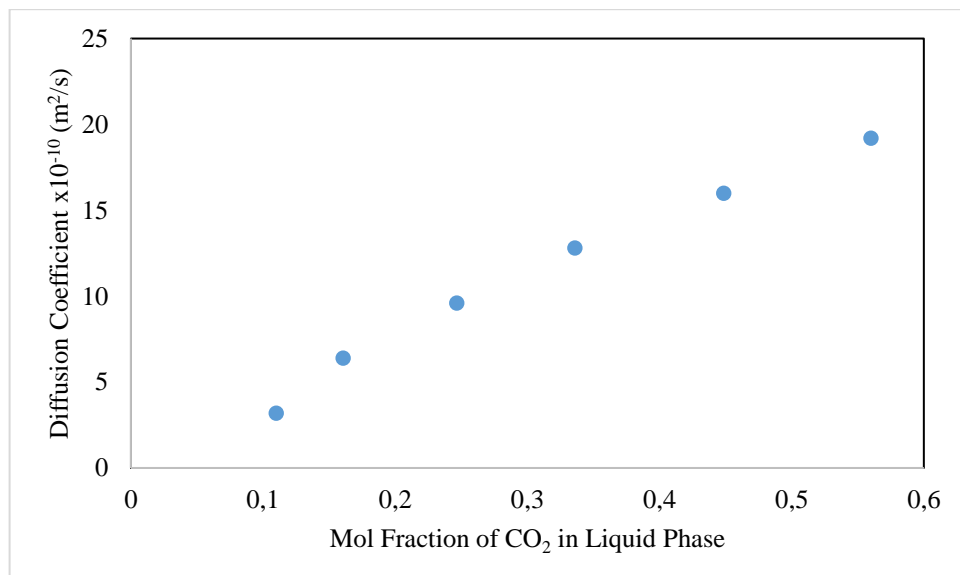

Figure 4.15. Liquid Phase Mutual Diffusion Coefficients in CO_2-PEG 400 System at 80 bar, 313. 15 K

5. CONCLUSIONS

The solubilities of CO_2 in PEG 400 at different pressures (30-80 bar) and temperatures (313.15 and 323.15 K) are determined. We have found that the solubilities increase with pressure and decrease with temperature. Although 313.15 K has given higher solubilities compared to 323.15 K, the differences at different pressures are not found to be high contrary to those reported by Daneshwar et al. The results obtained at 313.15 K have better matched with the data presented by Gourguillon et al.

The mutual diffusivities in PEG 400-CO_2 process at 313.15 K and 80 bar are also determined using a CFD model fitted to time-dependent solubility data. The increase in the liquid volume and the decrease in the molar volume are taken into account. The diffusivities have increased more than 6 times as carbon dioxide dissolves in the liquid polymer.

The repeat experiments for the solubilities are also carried out and comparable results are obtained. However, at 313.15 K, at a pressure of 40 bar, and at 323 K at pressures of 30 and 40 bar, the data can be better consolidated.

The following directions are recommended for future work:

- Increasing the temperature interval is worth examining since the increase in the difference in CO_2 solubilities will cause more significant changes in diffusivities at equilibrium CO_2 mole fraction.
- The diffusivities of CO_2 in PEGs of different molecular weights can be studied.
- Thermodynamic models using different equations of state and mixing rules can be developed for these systems.
- The diffusion coefficient of carbon dioxide in polyethylene glycol and ionic liquid mixtures can be investigated as multicomponent diffusion since some applications of these systems have started to emerge.

REFERENCES

1. Chen J, Spear SK, Huddleston JG, Rogers RD. *Green Chemistry*, 2005: 64.

2. Knez Hrnci M, Markoci E, Trupej N, Skerget M, Knez Z. Investigation of thermodynamic properties of the binary system polyethylene glycol/CO_2 using new methods. *The Journal of Supercritical Fluid*. 2014: 50-58.

3. Cooper AI. Synthesis and processing of polymers using supercritical carbon dioxide. *Journal Material Chemistry*. 2000: 207-34.

4. Nalawade SP, Picchioni F, Janssen LPBM. Supercritical carbon dioxide as a green solvent for processing polymers. *Progress Polymer Science*. 2006: 19-43.

5. Heldebrant DJ, Witt H, Walsh S, Ellis, T, Rauscher J, Jessop PG. Liquid polymers as solvents for catalytic reductions. *Green Chemistry*. 2006: 807.

6. Kordikowski A, Schenk AP, Van Nielen RM, Peters CJ. Volume expansions and vapor-liquid equilibria of binary mixtures of a variety of polar solvents and certain near-critical solvents. *Journal Supercritical Fluid*. 1995: 205.

7. Sekerci-Cetin M, Emek ÖB, Yildiz EY, Unlusu B. Numerical study of the dissolution of carbon dioxide in an ionic liquid. *Chemical Engineering Science*. 2016: 173-179.

8. Chen C, Even MA, Wang J, Chen Z. Sum frequency generation vibrational spectroscopy studies on molecular conformation of liquid polymers poly(ethylene glycol) and poly(propylene glycol) at different interfaces. *American Chemical Society*. 2002: 9130-9135.

9. Heldebrant DJ, Witt HN, Walsh SM, Ellis T, Rauscherb J, Jessop PG. Liquid polymers as solvents for catalytic reductions. *The Royal Society of Chemistry*. 2006: 807-815.

10. Obermeier B, Wurm F, Mangold C, Frey H. Multifunctional poly(ethyleneglycol)s. *Angewandte Chemie International Edition*. 2011: 7988-7997.

11. Wang H, Panic M, MP Biomedicals, 2018, [cited 2018 24 April] . Available from: http://www.mpbio. com/product.

12. Chemical Industry, Polyethylene glycol [cited 2018 20 May]. Available from: chemindustry.ru.

13. Winger M, De Vries AH, Gunsteren WF. Force-field dependence of the conformational properties of α,ω-dimethoxypolyethylene glycol. *Molecular Physics*. 2009: 1313-1321.

14. Weidner E, Wiesmet V, Knez Z, Skerget M. Phase equilibrium (solid-liquid-gas) in polyethyleneglycol carbondioxide systems. *Journal of Supercritical Fluids*. 1997: 139-147.

15. Kerton MF. Alternative solvents for green chemistry. *The Royal Society of Chemistry*. 2009: 170.

16. McHugh MA, Krukonis V. *Encyclopaedia of Polymer Science and Engineering*. New York, Wiley-Interscience, 1989.

17. D'souzaa AA, Shegokarb R. Polyethylene glycol (PEG): a versatile polymer for pharmaceutical applications. *Expert Opinion on Drug Delivery*. 2016: 1257-75.

18. Knox D. Solubilities in Supercritical Fluids. *Pure Applied Chemistry*. 2005: 513-530.

19. Cansell F, Rey S, Beslin P. Thermodynamic aspects of supercritical fluid processing: applications to polymers and wastes treatment. *Oil & gas science and technology – review*. 1998: 71-98.

20. Heller T, The Deplorable Climate Change, 2016, [cited 2016 10 August]. Available from: https://realclimatescience.com/2016/08/greenhouse-gases-warm-the-atmosphere/

21. Kendall JL, Canelas DA, Young JL, De Simone JM. Polymerizations in supercritical carbon dioxide. *Chemical Reviews*. 1999: 543-64.

22. Hyatt JA. Liquid and supercritical carbon dioxide as organic solvents. *Journal Organic Chemistry*. 1984: 5097-101.

23. Mchugh MA, Krukonis VJ. Supercritical fluid extraction. *Supercritical of Technology*. 1994.

24. Jessop PG, Leitner W. *Chemical synthesis using supercritical fluids*. New york: Wiley WCH; 1999.

25. Akien GR, Poliakoff M.A critical look at reactions in class I and II gas-expanded liquids using CO_2 and other gases. *Green Chemistry*. 2009:1083-1100.

26. Heldebrant DJ, Witt H, Walsh S, Ellis T, Rauscher J, Jessop FG. Liquid polymers as solvents for catalytic reductions. *Green Chemistry.* 2006: 807.

27. Iguchi M, Hiraga Y, Kasuya K, Aida TM, Watanabea M, SatoaY, Smith Jr RL. Viscosity and density of poly(ethylene glycol) and its solution with carbon dioxide at 353.2K and 373.2K at pressures up to 15 Mpa. *The Journal of Supercritical Fluids*. 2015: 63-73.

28. Subramaniam B, Scurto AM, Hutchenson KW. Gas expanded liquids and near-critical media Green Chemistry and Engineering. Washington DC: American Chemical Society, 2009 .

29. Tomasko DL, Hongbo L, Liu D, Han X, Wingert MJ, Lee LJ, Koelling KW. A review of CO_2 applications in the processing of polymers. *Industrial Engineering Chemistry and Research*. 2003: 6431-6456.

30. Kazarian SG. Polymer processing with supercritical fluids. *Polymer Science Series C*. 2000: 78.

31. Daneshvar M, Kim S, Gülari E. High pressure phase equilibria of polyethylene glycol-CO_2 systems. *Journal Physical Chemistry*. 1990: 2124-2128.

32. Gourgouillon D, Nunes M. High pressure phase equilibria for polyethylene glycol+CO_2 ; experimental results and modeling. *Physical Chemistry and Chemical Physics*. 1999: 5369-75.

33. Li J, Ye Y, Chen L, Qi,Z. Solubilities of CO_2 in poly(ethylene glycols) from (303.15 to 333.15) K. *Journal of Chemical and Engineering Data*. 2011.

34. Glatzel T, Litterst C, Cupelli C, Lindemann T, Moosmann C, Niekrawietz R, Streule W, Zengerle R, Koltay P. Computational fluid dynamics (CFD) software tools for microfluidic applications − A case study. *Science Direct*. 2008: 218-235.

35. Çengel YA, Cimbala JM. Computational fluid dynamics. *Fluid Mechanics Fundamentals and Applications*. 2006: 818-820.

36. Wendt J F, *Computational Fluid Dynamics: An Introduction*, Splinger, 2009.

37. Teledyne ISCO Syringe Pumps, 2018, [cited 2018 10 August]. Available from: 100DX_Syringe_Pump_datasheet.pdf.

38. Jerguson Product of Clark-Reliance, 2018, [cited 2018 10 August]. Available from: https://www.jerguson.com/company_products/armored-level-gauges/.

39. Measurements with the cathetometer, Available from: http://electro.chem.elte.hu:5080/ Laboranyag/Chemistry_BSc_English_Group/BLOCK_06/AAA_Measurements%20wit h%20the%20cathetometer.pdf.

APPENDIX A: REPEAT EXPERIMENTS FOR THE SOLUBILITY OF CO_2 IN PEG 400 AT DIFFERENT PRESSURES (30-80 BAR) AND 313.15 K

Figure A.1 shows that the solubilities obtained from the repeat experiments generally compare well with the original results.
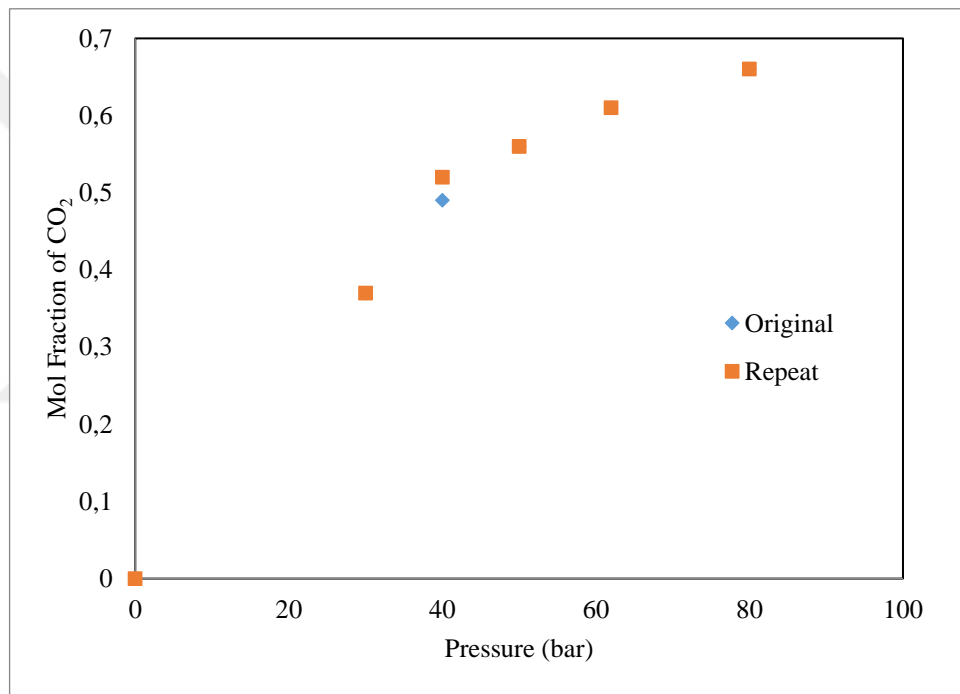

Figure A.1. Comparison of Mol Fraction versus Pressure in 313.15 K

Figures A.2-A.5 show the collected data points during the experiments.
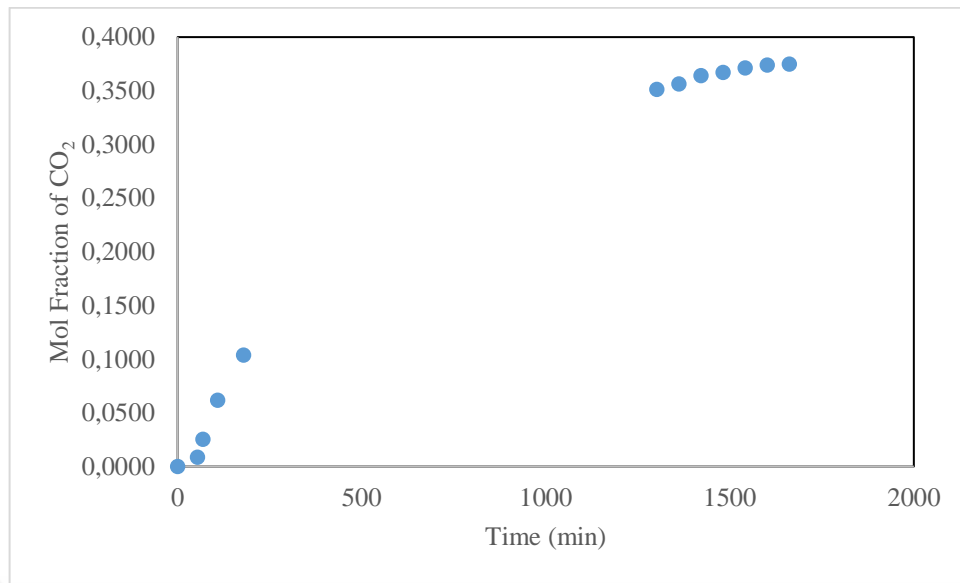
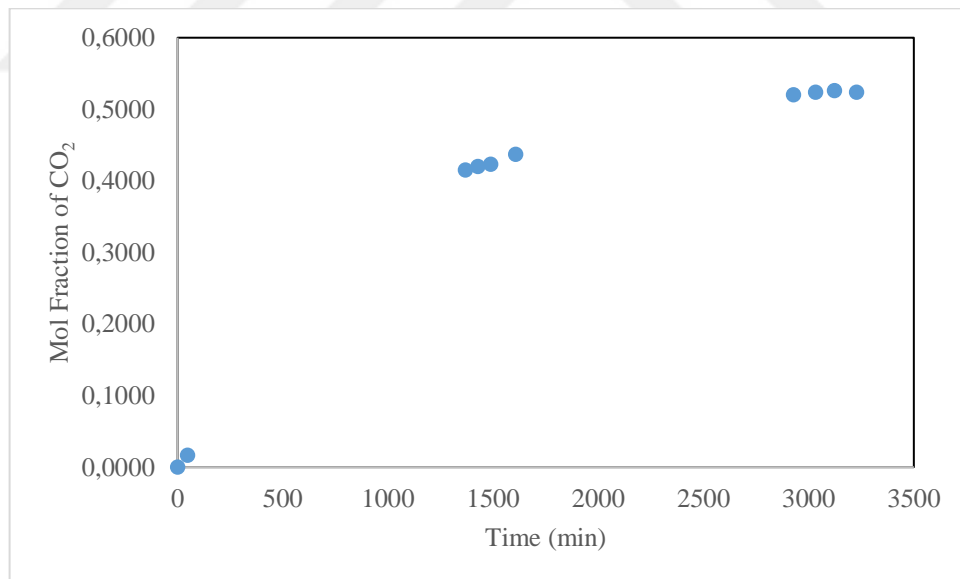Figure A.2. Change in Liquid Mol Fraction of CO_2 with Time at 30 bar, 313.15 K

Figure A.3. Change in Liquid Mol Fraction of CO_2 with Time at 40 bar, 313.15 K
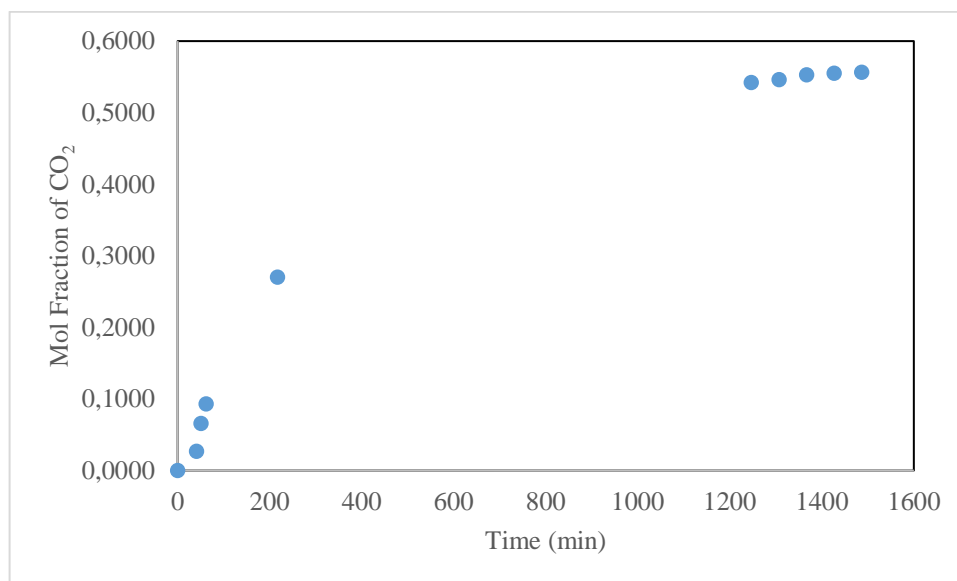
Figure A.4. Change in Liquid Mol Fraction of CO_2 with Time at 50 bar, 313.15 K
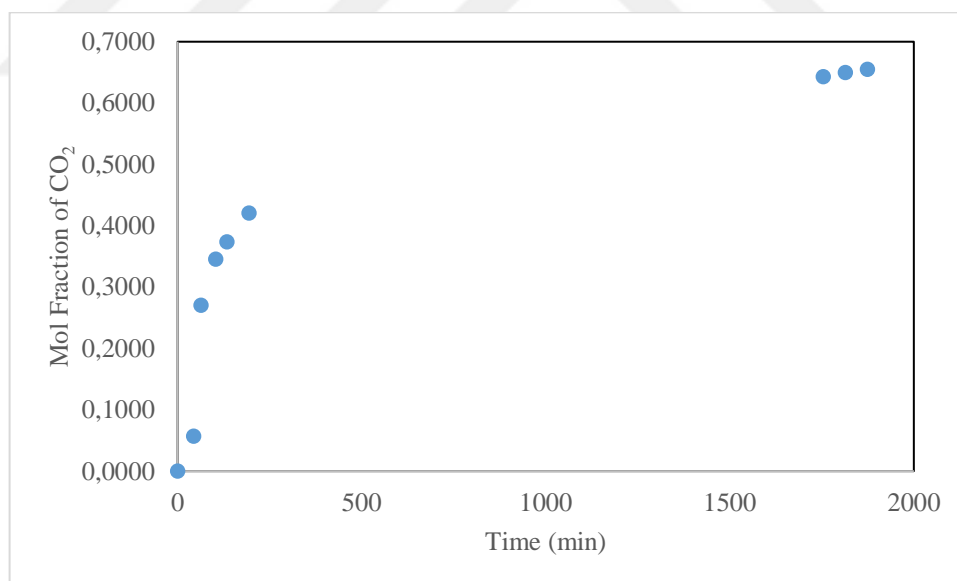
Figure A.5. Change in Liquid Mol Fraction of CO_2 with Time at 62 bar, 313.15 K

APPENDIX B: REPEAT EXPERIMENTS FOR THE SOLUBILITY OF CO_2 IN PEG 400 AT DIFFERENT PRESSURES (30-80 BAR) AND 323.15 K

Figure B.1 shows a comparison between the results obtained from the original and repeat experiments. Figures B2-B5 show the collected data.
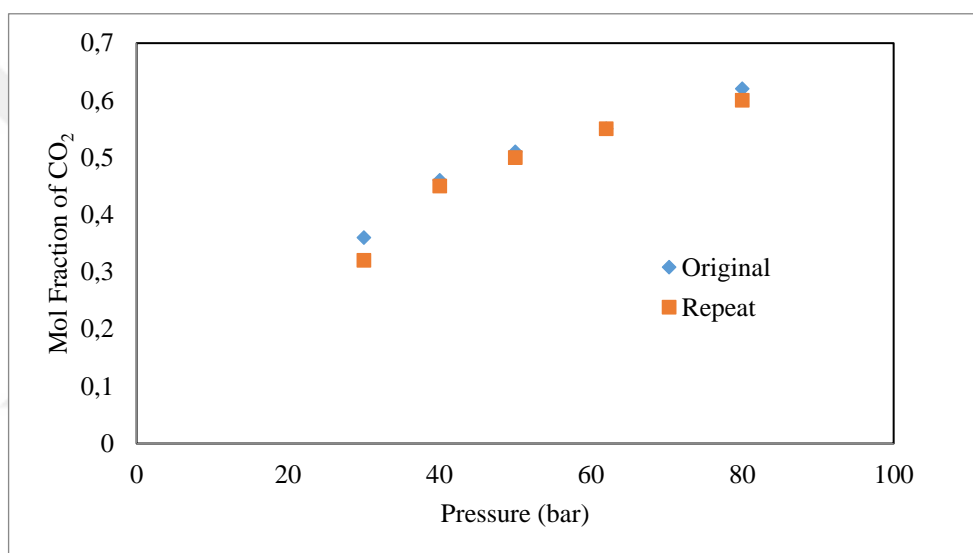

Figure B.1. Comparison of Mol Fraction versus Pressure in 323.15 K

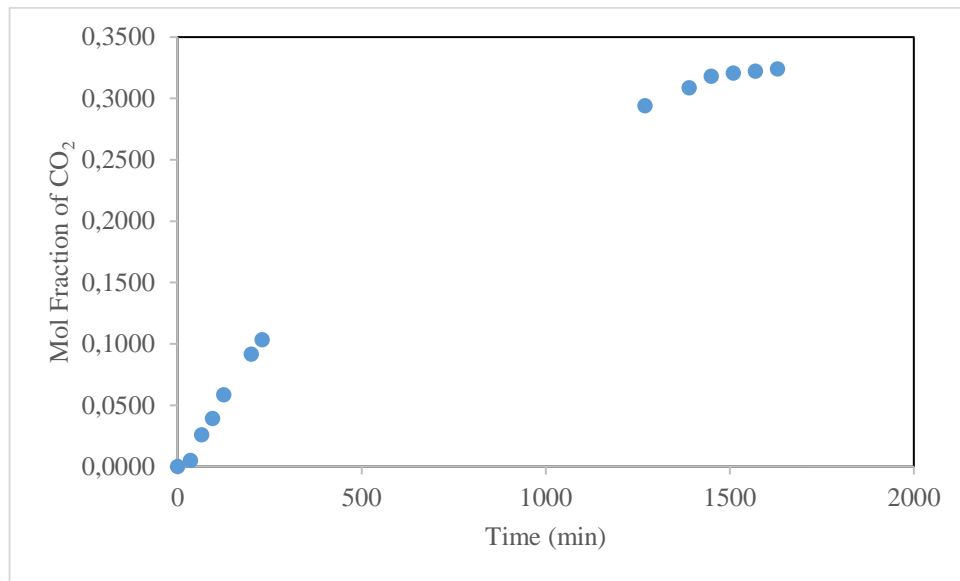Figures B.2-B.5 show the collected data points during the experiments.

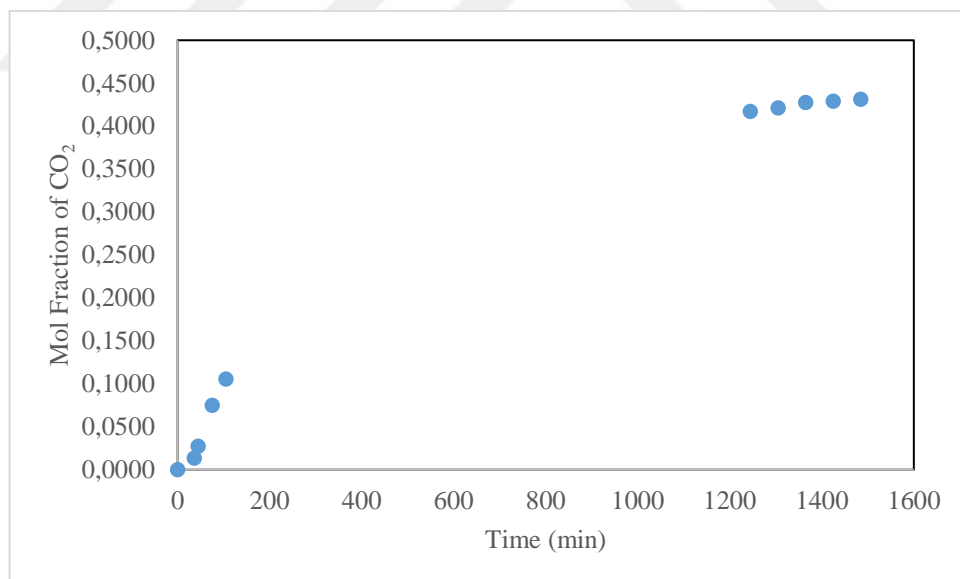Figure B.2. Change in Liquid Mol Fraction of CO_2 with Time at 30 bar, 323.15 K

Figure B.3. Change in Liquid Mol Fraction of CO_2 with Time at 40 bar, 323.15 K
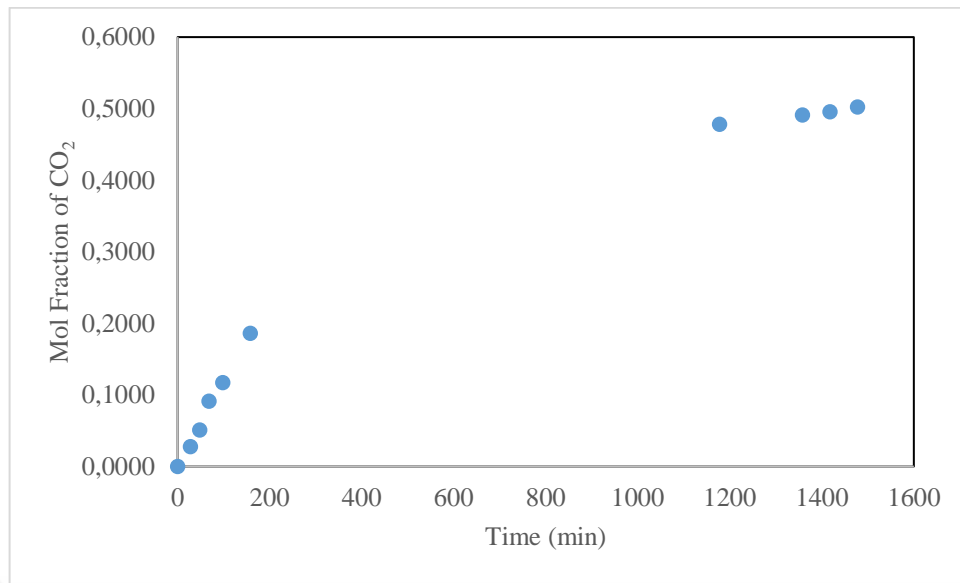
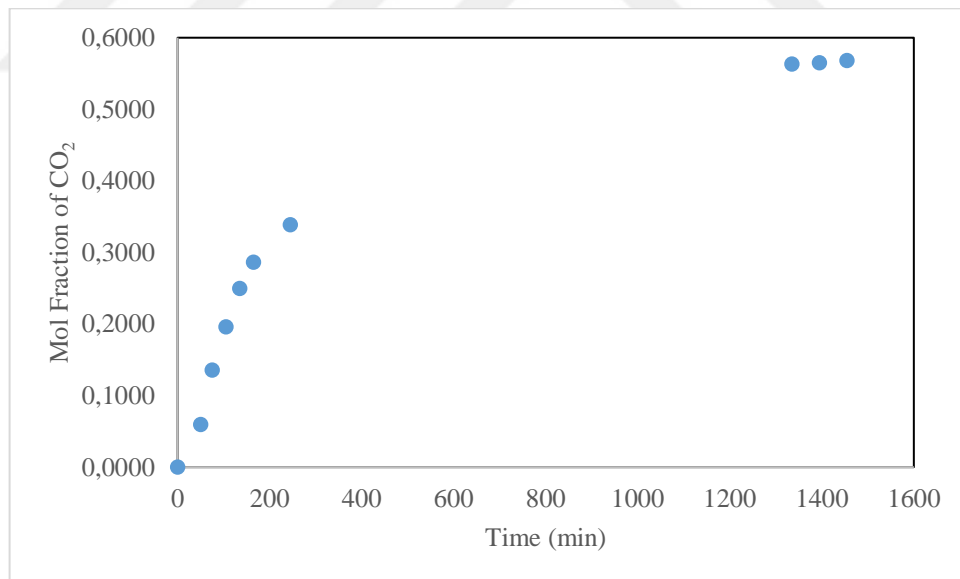Figure B.4. Change in Liquid Mol Fraction of CO_2 with Time at 50 bar, 323.15 K

Figure B.5. Change in Liquid Mol Fraction of CO_2 with Time at 62 bar, 323.15 K

APPENDIX C. REPEAT OF PEG 400 – CO$_2$ SYSTEM AT 313.15 K AND 80 BAR

The experimental data is shown in Table C.1 The data obtained from the repeat and original experiments are comparable as shown in Figure C.1.

Table C.1 The Experimental Data For 80 bar, 313.15 K

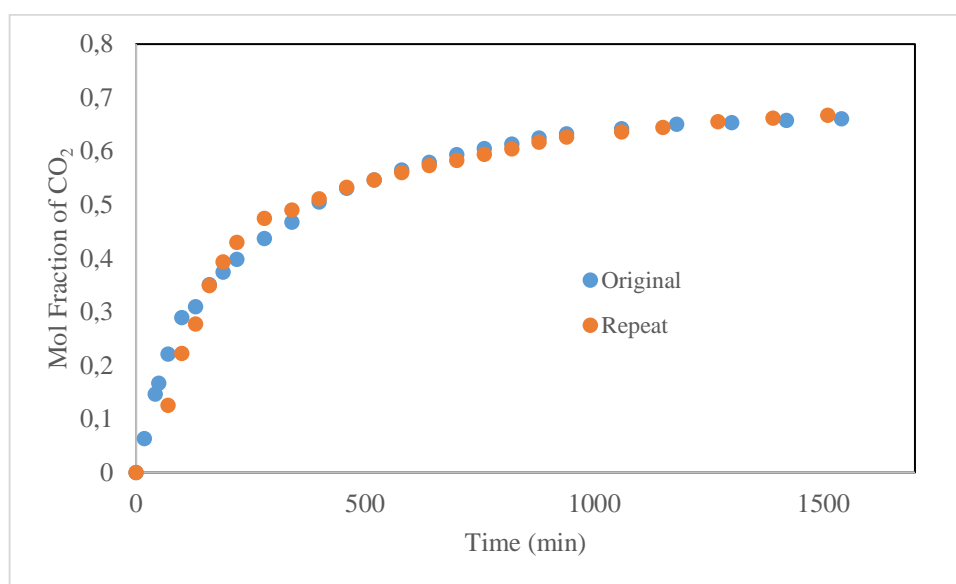|	
Mass of the PEG 400 in the system	8,0854 g
Volume of carbon dioxide loaded to the system	152.12 ml
Initial volume of carbon dioxide in syringe pump	239.09 ml
Final volume of carbon dioxide in syringe pump	83.17 ml
Increase in liquid level	3.65 mm
Pressure of the system during the experiment	80 bar
Temperature of the system during the experiment	313.15 K

Figure C.1. Mol Fraction of CO_2 Change with Time at 80 bar, 313.15 K

APPENDIX D: SAMPLE CALCULATION FOR EQUILIBRIUM MOLE FRACTION AT 313.15 K AND 80 BAR

A sample calculation is determined for equilibrium mole fraction at 313.15 K and 80 bar ;

- Mass of the ionic liquid in the system: 8.0854 g
- Volume of carbon dioxide loaded to the system: 152.12 ml
- Initial volume of carbon dioxide in syringe pump: 239.09 ml
- Final volume of carbon dioxide in syringe pump: 83.2 ml
- Pressure of the system during the experiment: 80 bar
- Temperature of the system during the experiment: 313.15 K
- Increase in the liquid level at equilibrium: 3.65 mm

$$n_{i,isco} = n_{CO_2} + n_{f,isco} + n_{f,jerguson} \tag{D.1}$$

Final volume of carbon dioxide at gas phase in Jerguson: 152.12– (5.55*0.365)= 150.09 ml

Volume of carbon dioxide dissolved in the liquid: 239.09-83.2-150.09=5.8 ml

Number of moles of carbon dioxide in the liquid: 5.8/150.5= 0.039 mole

Number of moles of the liquid: 8.0854/400= 0.0202 mole

150.5 cm^3/mol is the molar volume of carbon dioxide at ~80 bar 313.15 K. 400 is the molecular weight of the PEG 400 and the equilibrium mole fraction of carbon dioxide in the liquid is equal to 0.66.